MedChemComm

Accepted Manuscript

This article can be cited before page numbers have been issued, to do this please use: V. S. Koneni, L. R. Singh, M. Shameem, S. Shakya, A. Kumar, T. S. Laxman, S. Krishna, M. I. Siddiqi, R. S. Bhatta and D. Banerjee, *Med. Chem. Commun.*, 2016, DOI: 10.1039/C6MD00447D.

ROYAL SOCIETY OF CHEMISTRY

www.rsc.org/medchemcomm

View Article Online
DOI: 10.1039/C6MD00447D

Journal Name

ARTICLE

Design, synthesis and anticancer activity of dihydropyrimidinone-semicarbazone hybrids as potential Human DNA Ligase1 inhibitors‡

Received 00th January 20xx,
Accepted 00th January 20xx

DOI: 10.1039/x0xx00000x

www.rsc.org/

Koneni V. Sashidhara,*[a] L. Ravithej Singh,[†a] Mohammad Shameem,[†b] Sarika Shakya,[a] Anoop Kumar,[a] Tulsankar Sachin Laxman,[c] Shagun Krishna,[b] Mohammad Imran Siddiqi,[b] Rabi S. Bhatta[c] and Dibyendu Banerjee*[b]

A series of new dihydropyrimidinone-semicarbazone hybrids were successfully synthesised by integrating regioselective multicomponent reaction with the pharmacophore hybridization approach. All the synthesised compounds were evaluated for their hLig1 inhibition potency and most of them were found to be good to moderately active. Out of the tested derivatives, compound **6f** showed selective anti-proliferative activity against HepG2 cells in a dose-dependent manner with an IC_{50} value 10.07±1.2. It also reduced cell survival at ≤20 µM concentration. Further, analysis of treated HepG2 cells lysate by western blot assay showed increased γH2AX levels and upregulation of p53, leading to apoptosis. *In-silico* docking results explain binding modes of compound **6f** to DNA-binding domain of hLig1 enzyme thereby preventing its nick sealing activity. In addition, the favourable pharmacokinetic properties suggest that this new class of hLig1 inhibitors could be promising leads for further drug development.

1. Introduction

DNA replication is a fundamental molecular process that occur in dividing cells to ensure the transmission of genome to new generation with exact nucleotide sequence.[1] Genetic defects in the replication, repair, and recombination of DNA are major cause of genomic instability that can lead to unregulated cellular proliferation and cancer. Approximately one mutation is introduced during the replication of every ten billion base pairs. It is estimated that among various kinds of DNA damages, single strand breaks (SSBs) are the most common type of DNA damage that arise in the cell.[2] If not properly repaired, it can pose a threat to genomic stability and cell survival. DNA ligases play important roles during DNA replication, repair, and recombination processes.[3] They catalyze the nick joining by phosphodiester bond formation in double stranded DNA. Mammalian cells have three types of ATP-dependant DNA ligases, *viz*., Ligase1, Ligase3, and Ligase4.

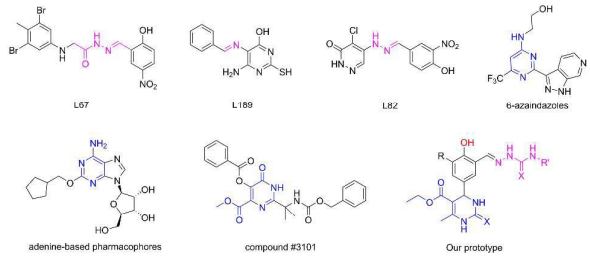

Fig. 1. Chemical structure of some DNA ligase inhibitors reported in literature and our designed prototype.

These DNA ligases have conserved catalytic core to accomplish the ligation reaction *via* a common mechanism.[4] Among them, hLig1 is a major replicative enzyme which joins the Okazaki fragments during DNA replication. It also joins the SSBs in DNA generated by DNA glycosylases enzyme during base excision repair.[5] Thus, DNA ligation is an essential process required by all cells during replication. Defects in the nick joining activity of hLig1 can cause greater genomic impermanence and hypersensitivity to DNA damaging agents leading to cellular lethality.[6] Further, elevated levels of hLig1 have been found in various cancer cells such as breast, lung, and ovarian cancer cells. Sun *et al*., found high levels of hLig1 in human tumors compared to normal benign tissues and normal peripheral lymphocytes.[7] Recent studies have identified ligase inhibitors to obstruct the ligation activity and specifically kill the cancer cells.[8]

In recent years, many therapeutic agents have been discovered, intended to target DNA replication for the

[a]*Medicinal and Process Chemistry Division, CSIR-Central Drug Research Institute, BS-10/1, Sector 10, Jankipuram Extension, Sitapur Road, Lucknow, 226031, India.*
[b]*Molecular and Structural Biology Division, CSIR-Central Drug Research Institute, BS-10/1, Sector 10, Jankipuram Extension, Sitapur Road, Lucknow, 226031, India.*
[c]*Pharmacokinetics and Metabolism Division, CSIR-Central Drug Research Institute, BS-10/1, Sector 10, Jankipuram Extension, Sitapur Road, Lucknow, 226031, India.*
† *These authors contributed equally.*
* *Corresponding authors,* Fax: +91 522 2771942; Tel: +91 9919317940; E-mail: sashidhar123@gmail.com; kv_sashidhara@cdri.res.in; d.banerjee@cdri.res.in
‡The authors declare no competing interests.
Electronic Supplementary Information (ESI) available: [details of any supplementary information available should be included here]. See DOI: 10.1039/x0xx00000x

View Article Online
DOI: 10.1039/C6MD00447D

treatment of malignant tumors.[9] Melphalan and chlorambucil alkylate the guanine base in genetic material thereby prevent DNA replication. World Health Organisation listed these drugs among the essential medicines, however, they associated with neuronal and hepatotoxicity.[10] Another anticancer agent, 5-flurouracil (5-FU) interrupts replication process by inhibiting the synthesis of thymidine nucleoside, with frequent side effects such as cardio toxicity and diarrhea.[11] DNA intercalating agent, doxorubicin, interferes replication process by virtue of topoisomerase inhibition with adverse effects. In light of the above limitations for the existing drugs, the need of new anticancer agents is an unmet medical need.[12]

Interestingly, few attempts have been made to develop bacterial DNA ligase inhibitors. For example, Menchon et. al. revealed the bacterial DNA ligase inhibitory potency of compound #3101 (Fig. 1) by computational, biophysical and biochemical analysis.[13] While, other research groups reported 6-azaindazoles[14] and adenine-based[15] pharmacophores as promising DNA ligase inhibitors that can be developed for bacterial infections.

Previous studies from our lab have shown that inhibition of hLig1 preferentially kills some cancer cells over normal ones.[16a] Therefore, hLig1 could be a possible therapeutic target for developing novel anticancer agents. Chen *et. al*. identified the ability of compounds L67, L82, and L189 with selective hLig1 inhibition in cancer cell without affecting normal cells (Fig. 1). The docking of these compounds to the DNA binding site of hLig1 has been described elsewhere.[16b] By careful inspection of the docked complexes of these three compounds, we have identified that hydrazine-carboxamide moieties are contributing significantly to the interactions of these compounds with DNA binding residues of the hLig1 crystal structure. Therefore, we have decided to explore these moieties more extensively. Consequently, in an effort to synthesise new class of hLig1 inhibitors, we rationally designed a new class of dihydropyrimidinone-semicarbazonehybrids by combining two pharmacophores[17] in order to increase the binding interactions of ligand to the targeted protein.[18]

2. Chemistry

The synthetic route for the designed molecules is shown in Scheme 1. The Duff formylation reaction on 2-alkyl phenols (**1a-b**) in the presence of hexamethylenetetramine (HMTA) and trifluoracetic acid (TFA) followed by hydrolysis using 10% aq. H_2SO_4 solution gave 5-alkyl-4-hydroxyisophthalaldehyde intermediates (**2a-b**).[19] Then, these isophthalaldehyde intermediates undergo reaction with urea/thiourea and ethyl acetoacetate in the presence of glacial acetic acid as a solvent to give regioselective dihydropyrimidinone derivatives (**3a-c**) in good yields.[20] On the other hand, substituted N-phenylhydrazine-carboxamides (**5a-e**) were synthesized by using suitably substituted phenyl isocyanates with hydrazine hydrate in dichloromethane (DCM) at 0 °C.[21] Synthesis of N-phenylhydrazine-carbothioamide derivatives (**5f-h**) was carried out by literature procedure.[22] Finally, the target compounds were synthesized by condensation of dihydropyrimidinone

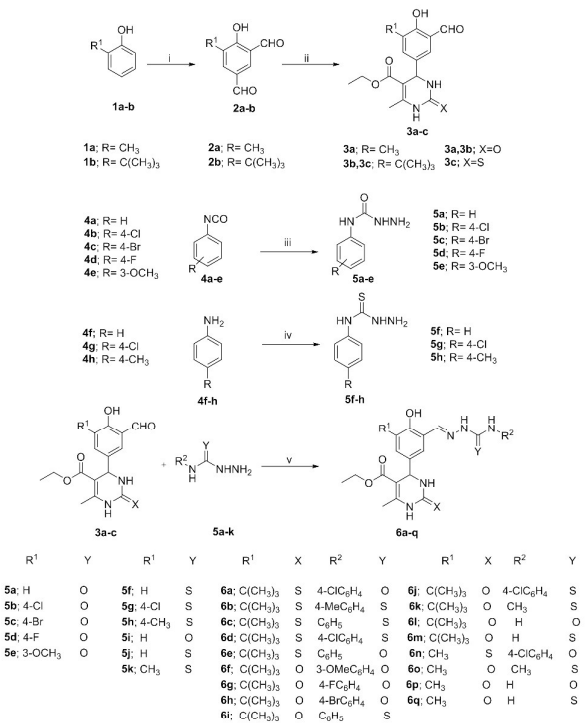

5a; H	O	**5f**; H	S	**6a**; $C(CH_3)_3$	S	4-ClC_6H_4	O	**6j**; $C(CH_3)_3$	O	4-ClC_6H_4	S
5b; 4-Cl	O	**5g**; 4-Cl	S	**6b**; $C(CH_3)_3$	S	4-MeC_6H_4	S	**6k**; $C(CH_3)_3$	O	CH_3	S
5c; 4-Br	O	**5h**; 4-CH_3	S	**6c**; $C(CH_3)_3$	S	C_6H_5	S	**6l**; $C(CH_3)_3$	O	H	O
5d; 4-F	O	**5i**; H	O	**6d**; $C(CH_3)_3$	S	4-ClC_6H_4	S	**6m**; $C(CH_3)_3$	O	H	S
5e; 3-OCH_3	O	**5j**; H	S	**6e**; $C(CH_3)_3$	S	C_6H_5	O	**6n**; CH_3	S	4-ClC_6H_4	O
		5k; CH_3	S	**6f**; $C(CH_3)_3$	O	3-$OMeC_6H_4$	O	**6o**; CH_3	O	CH_3	S
				6g; $C(CH_3)_3$	O	4-FC_6H_4	O	**6p**; CH_3	O	H	O
				6h; $C(CH_3)_3$	O	4-BrC_6H_4	O	**6q**; CH_3	O	H	S
				6i; $C(CH_3)_3$	O	C_6H_5	S				

Scheme 1: Synthesis of dihydropyrimidinone-semicarbazone hybrids. Reagents and Conditions: (i). a) TFA, 110 °C, 6-8 h; b) 10% H_2SO_4; (ii). urea/thiourea, ethylacetoacetate, AcOH, reflux, 2 hours; (iii). phenylhydrazinecarboxamide derivatives, ethanol, rt stirring for 3-4hours; (iv) a) CS_2, NaOH, DMF, 1h, 20-35 °C; b) N_2H_2-H_2O, 1h, 60-70 °C; (v) Ethanol, 2-3 h stirring.

with substituted N-phenylhydrazinecarboxamides/carbothioamide in ethanol to furnish the respective dihydropyrimidinone-semicarbazone hybrid compounds (**6a-q**). The structures of all the new compounds were elucidated by ^{1}H NMR, ^{13}C NMR, mass spectrometry, and IR spectroscopy (see Supplementary info.).

3. Results and Discussion

3.1. Dihydropyrimidinone-semicarbazone hybrids inhibit hLig1 activity and induce cell death

All the newly synthesised compounds were tested for hLig1 nick joining activity at single dose of 100 µM concentration. Effect of seventeen final derivatives (**6a**-**q**) and two intermediates (**3a**-**b**) was evaluated in terms of both %ligation and % inhibition. Interestingly, all the compounds showed hLig1 inhibition at tested concentration, whereas compounds **3a-b** were comparatively less effective. After confirming the ligase inhibition efficacy, we assessed the cytotoxic potential of newly synthesised compounds on HepG2, A549, HCT-116, DLD-1, and MDAMB-231 cancerous cell lines along with HEK-293 normal human cell lines at 10 µM concentration. Out of seventeen derivatives **6a**, **6b**, **6c**, **6d**, **6f**, **6h**, **6i**, **6j**, and **6n** induce cell death in cancer cell lines. Interestingly, compound **6f** selectively inhibited HepG2 cell growth with minimal toxicity towards normal cell lines as shown in table **1**. These prominent

View Article Online
DOI: 10.1039/C6MD00447D

Table 1: % inhibition of hLig1 activity and % cell death of synthesized compounds (**6a-q**)

Compound No.	hLig1 activity at 100 µM		% cell death					
	% Ligation	% Inhibition	[a]HepG2	[b]A549	[c]HCT-116	[d]DLD-1	[e]MDAMB-231	[f]HEK-293
6a	22.9	77.1	81.3	54.0	63.3	17.1	13.8	65.7
6b	31.1	68.9	23.5	9.3	50.5	45.7	3.3	40.2
6c	33.2	66.8	26.5	29.6	49.9	67.6	26.1	54.1
6d	20.6	79.4	28.9	24.5	57.8	15.5	17.3	52.7
6e	19.1	80.9	26.0	26.8	17.9	17.6	7.0	53.3
6f	17.4	82.7	52.2	18.1	18.2	29.4	28.4	11.7
6g	15.3	84.7	37.1	39.3	17.5	19.1	43.7	46.8
6h	16.0	84.0	65.3	45.3	57.2	60.2	44.8	35.3
6i	12.0	88.1	43.0	48.7	43.2	30.0	50.4	48.3
6j	19.1	80.9	78.9	53.3	82.5	43.0	83.6	53.1
6k	19.2	80.8	23.7	27.3	22.5	34.1	29.7	24.6
6l	22.4	77.6	0.7	9.1	2.6	19.9	18.4	14.0
6m	19.6	80.4	11.1	17.0	7.8	5.5	21.1	17.0
6n	13.4	86.7	22.8	12.8	50.8	1.0	20.2	42.6
6o	19.6	80.4	33.1	14.0	17.7	18.1	31.0	22.7
6p	35.7	64.3	9.7	7.0	4.3	-3.0	13.9	15.7
6q	15.9	84.1	23.3	4.7	1.3	6.2	10.7	6.7
3a	23.1	76.9	18.3	34.7	5.7	14.7	32.5	9.2
3b	26.4	73.6	11.4	25.4	1.8	8.1	20.7	10.7

[a]Human Liver cancer cell line, [b]human lung carcinoma cell line, [c,d]human colon cancer cell lines, [e]breast cancer cell line, [f]human embryonic kidney cell line

results prompted us to choose compound **6f** for further investigation.

3.2. Compound 6f abolished the nick sealing activity of hLig1

The hLig1 catalyzes the joining of nicks or single strand breaks present on a DNA substrate. To test the ability of compound **6f** to inhibit the DNA nick sealing activity of purified hLig1 enzyme, we performed the DNA joining assay as described in methods section. We found that compound **6f** was able to inhibit ligation in a concentration-dependent manner (Fig. 2A and 2B). The IC_{50} value for compound **6f** (12.45 ± 0.89 µM) was calculated as that of concentration caused 50% inhibition of ligation.

3.3. Compound 6f binds directly with hLig1

We performed three different experiments to examine the binding specificity of compound **6f** with hLig1. First, we performed CD spectroscopy to determine the domain responsible for binding of compound **6f** with hLig1. Our result showed clear shift in the spectrum upon addition of compound **6f** to hLig1 or its DBD when compared to control (protein alone). Shift in the CD spectra of hLig1 and DBD proteins in the presence or absence of compound **6f** confirmed the binding of this molecule to DBD of hLig1 (Fig. 3A). Further, we performed fluorescence spectroscopy experiments that are based on quenching of the signal from aromatic amino acids containing intrinsic fluorescence property. The addition of compound **6f** to purified hLig1 resulted in significant decrease in the intrinsic fluorescence of both full-length hLig1 and DNA binding domain of the hLig1 protein, indicating inhibitor binding with the protein (see Fig. **S1** supplementary info.).

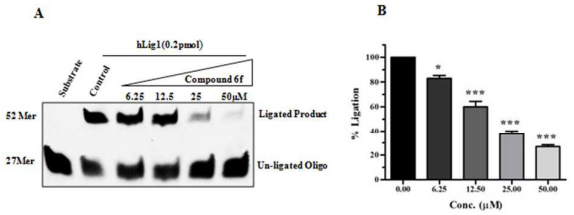

Fig. 2. Inhibitions of DNA nick joining activity of hLig1. **A)** The hLig1 (0.2 pmol) was incubated with nicked DNA substrate (1 pmol) in the absence or presence of inhibitor molecules. Ligated product (52 mer) was separated from unligated DNA (27 mer) by electrophoresis under denaturing conditions. Dose-dependent inhibition of nick sealing activity of compound **6f** was observed at various concentrations (50, 25, 12.5 and 6.25 µM). **B)** Bar graph showing the percent ligation in the presence of various concentrations of compound **6f**. Percentage of ligation was quantified by Image Quant LAS 4010 with control taken as 100 percent.

In addition, we also performed an *in-vitro* enzyme mobility shift assay to confirm the binding of compound **6f** with the hLig1-DNA complex. In the absence of an inhibitor, hLig1 can bind with DNA to form a secondary hLig1-DNA complex that runs higher up in a non-denaturing gel than either DNA or hLig1 alone (see Fig. **S2** supplementary info.). Interestingly, we found that there is a loss of signal from hLig1-DNA complex in the presence of compound **6f** in a concentration-dependent manner. This suggests the destabilization of hLig1-DNA complex upon treatment with inhibitor. Therefore, these results strongly suggest that compound **6f** binds directly with the hLig1 protein.[23]

3.4. Compound 6f does not interact with DNA

Since inhibition of ligation can occur either due to protein binding or DNA binding or both, we performed another experiment whereby we tested whether the compound has any affinity for the DNA.

View Article Online
DOI: 10.1039/C6MD00447D

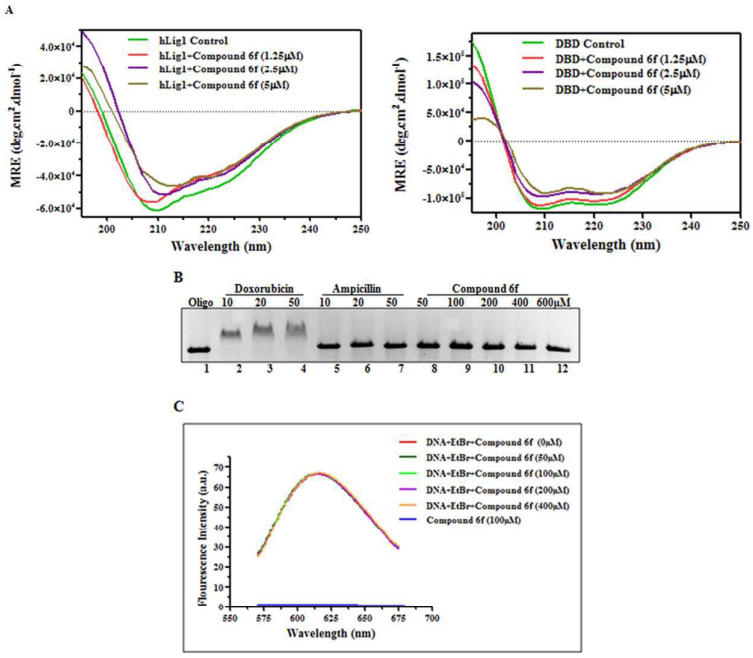

Fig. 3. Binding of compound **6f** to hLig1 enzyme. **(A)** CD Spectra of hLig1 and DBD in the presence or absence of compound **6f** inhibitor. (B) Intercalation of compound **6f** with DNA was evaluated by a gel-based assay. Linearized pUC18 plasmid was treated with different concentrations (50, 100, 200, 400 and 600 μM) of the inhibitor (Lanes 8 to 12). Doxorubicin (Lane 2 to 4) and Ampicillin (Lane 5 to 7) were used as positive and negative controls respectively for DNA intercalation. **(C)** Fluorescence-based EtBr displacement assay for compound **6f** shows no change in fluorescence up to 400 μM concentration.

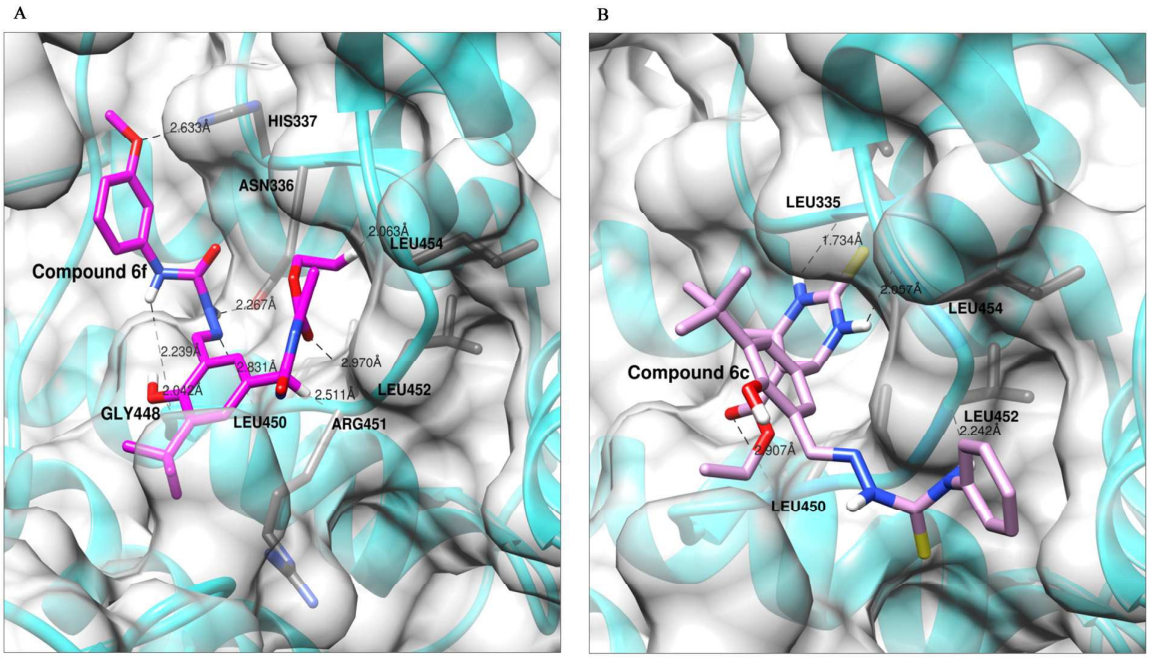

Fig. 4. The binding mode of compound **6f** (A) and **6c** (B) is shown in the DNA binding site of hLigI crystal structure 1X9N. The compound **6f** and **6c** are shown in magenta and pink sticks respectively; the interacting residues of protein are shown in grey sticks; black dashed lines represent the hydrogen bond with their respective length.

We performed a gel based DNA intercalation assay with linearized pUC18 plasmid DNA after incubating the DNA with increasing concentrations of compound **6f** for 30 min at 37 °C. We did not found any visible shift (up to 600 μM concentration) in the movement of DNA in the gel when compared to control. Doxorubicin and ampicillin were used in the experiment as positive and negative controls for DNA intercalation (Fig. 3B). These results indicate that compound **6f**

View Article Online
DOI: 10.1039/C6MD00447D

does not intercalate with DNA. Further, we confirmed the binding of compound **6f** with DNA by using a more sensitive fluorescence spectroscopy based ethidium bromide (EtBr) displacement assay. Our results demonstrated that compound **6f** did not cause any significant loss in fluorescence of EtBr up to 400 µM concentration (Fig. 3C). Taken together, our results demonstrate that compound **6f** does not interact with DNA. Therefore, inhibition of ligation occurs due to direct binding of compound **6f** with hLig1 and not due to DNA binding.

To elucidate the binding mode of these inhibitors, we have docked them into the DNA binding site of crystal structure of hLig1. We have obtained higher docking score for the compound **6f** against hLig1 structure, which might be able to rationalise its potent anti-ligation activity.

The predicted binding mode of the compound **6f** is presented in Fig. 4. As it can be seen from the Fig. 4A, the two NH groups of semicarbazone moiety are making hydrogen bonds with Asn336 and Gly448. Apart from this, Gly448 also interacting with hydrogen of phenolic hydroxyl group. Whereas, oxygen atom of 3-OMe substitution present on phenylhydrazine-carboxamide showing hydrogen bond with His337 amino acid. A hydrogen bond is also observed between imine nitrogen of semicarbazone and Leu450 residue. The dihydropyrimidinone ring is found close to the DNA-binding residues Arg451 along with Leu452 and involved in making hydrogen bond with these two residues. Additionally, compound **6f** is also interacting with Leu454 through a hydrogen bond. Most of these residues are reported to involve in making direct hydrogen bond with DNA in the crystal structure and they are assumed to play an important role in the binding of DNA to the protein hLig1. These interactions with the hLig1 may be responsible for contributing increased stability to the docked complex and can decipher the potent hLigI inhibition observed for compound **6f** in the *in-vitro* assays.

The binding mode of compound **6c** is presented in Fig. 4B, which has shown comparatively lower activity than active compound **6f** in the *in-vitro* assays. As shown in Fig. 4B, although the compound **6c** is forming few hydrogen bonds with residues Leu335, Leu450, Leu452, and Leu454. This difference in the binding mode of compound **6c** may explain the decreased potency of this analogue. The docking energies of these compounds are given in supplementary information.

3.5. Compound 6f prevent the proliferation of human cancer cell

To evaluate the effect of identified hLig1 inhibitor on cell viability, we performed the cell viability assay on various human cancer cell lines. Our results demonstrate that compound **6f** reduce the cell viability in HepG2 cancer cells significantly at 10 µM concentration while there is moderate cytotoxicity in other cancer cell lines. There is negligible cytotoxicity against normal Human Embryonic Kidney (HEK-293) cell line.

Further, we evaluated the cytotoxicity of compound **6f** against HepG2 cancer cells at various concentrations. Cell viability of HepG2 cells decreased (IC_{50} value 10.6±0.5µM) significantly with increasing concentration of compound **6f** molecule in a dose-dependent manner (Fig. 5A). These results denote that compound **6f** treatment reduces the cell viability of HepG2 cells by affecting the ligation activity of hLig1 enzyme which is a major replicative enzyme in mammalian cells. In addition, our clonogenic cell survival assay showed that treatment of HepG2 cells with compound **6f** causes cytotoxicty at 10µM concentration or above (Fig. 5B).

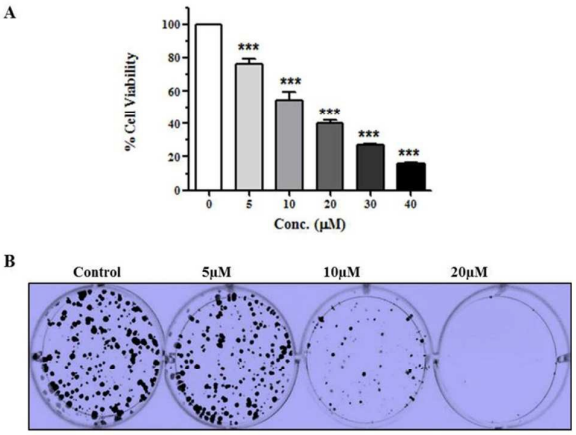

Fig. 5. Compound **6f** reduces cancer cell proliferation and survival. **(A)** HepG2 cells were treated with compound **6f** for 48 h and then subjected to MTT assay; the results are presented as bar graphs. **(B)** Cell survival assay was performed by treatment of HepG2 cells with compound **6f** at different concentrations (0, 5, 10 and 20 µM) for 48 h. After 48 h, cells were grown in their respective culture media for ten days. Cell colonies were stained with crystal violet, observed under the microscope.

3.6. Compound 6f suppress cell cycle progression and induce apoptosis in cancer cells

HepG2 cell lines were exposed to different concentrations of inhibitors for 48 h and then stained with Annexin V/ PI. Flow cytometry analysis showed that compound **6f** induces apoptosis in HepG2 cells significantly in a dose-dependent manner (Fig. 6A). We also examined the cell cycle progression in HepG2 cells after treatment with compound **6f** and found that it halts the cell cycle at a G_0/G_1 stage in a dose and time-dependent manner (Fig. 6B).

The hLig1 inhibitor-mediated mechanism of DNA damage would lead to an accumulation of DNA damage, leading to a reduction in cell proliferation and induction of apoptotic cell death. In order to measure an increase in DNA damage, we measured the level of γHA2X in cells treated with compound **6f** and confirmed that a higher level of γHA2X is present in treated cells (Fig. 6C). It is known that p53 protein plays an important role in regulating the cellular sensitivity to apoptosis in response to DNA damage and alter gene expression leading to cell cycle arrest, apoptosis or senescence.[24] We found that compound **6f** treatment in HepG2 cells upregulated p53 which leads to induction of apoptosis. Further, reduction in the level of proliferating cell nuclear antigen (PCNA) suggests that compound **6f** reduces cell proliferation (Fig. 6C). Therefore, our results confirm that alteration of these pathways in response to the compound **6f** treatment is a major cause of apoptotic cell death in HepG2 cells.

View Article Online
DOI: 10.1039/C6MD00447D

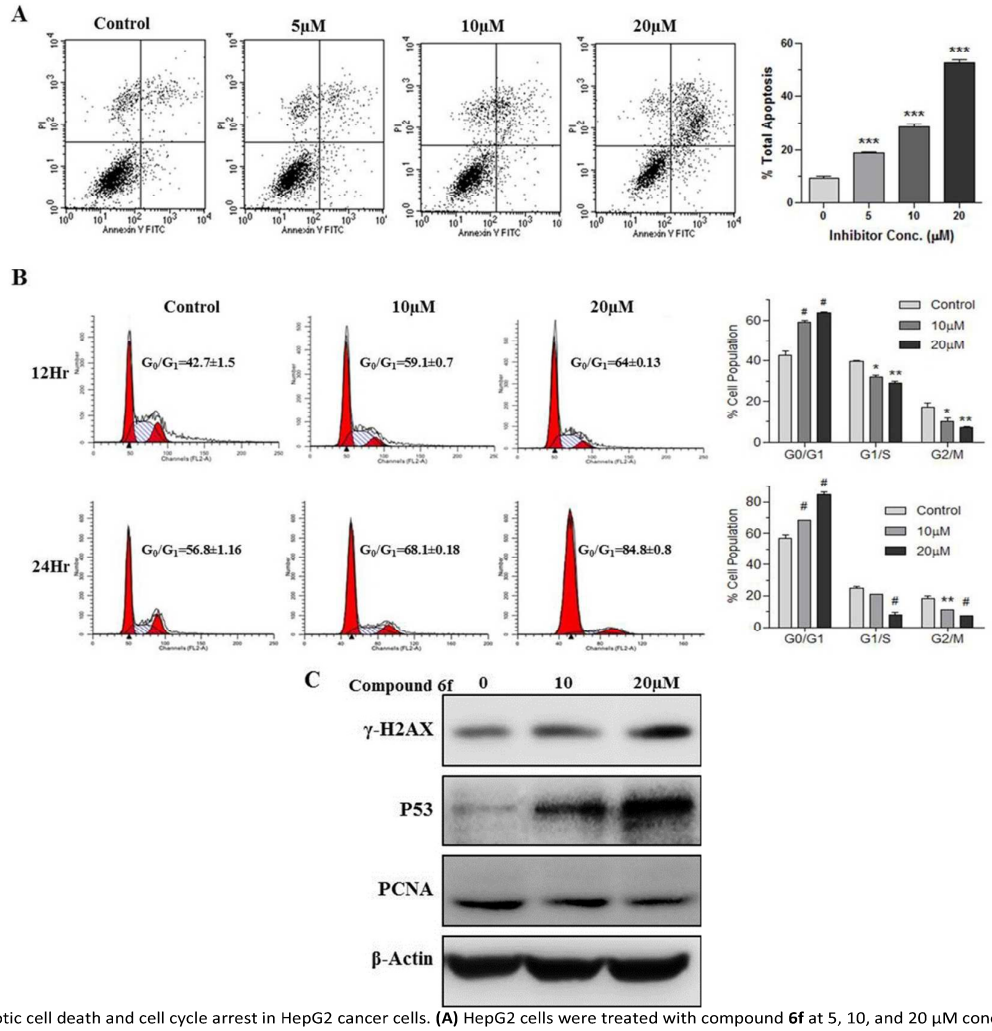

Fig. 6. Apoptotic cell death and cell cycle arrest in HepG2 cancer cells. **(A)** HepG2 cells were treated with compound **6f** at 5, 10, and 20 μM concentrations in complete culture media for 48 h. Apoptosis was quantified by staining with Annexin-V/PI followed by flow cytometry. The bar graph shows the percentage of cells undergoing apoptotic cell death. Data was analyzed by ANOVA and reported as mean ± standard error (SE) of the percentage of apoptosis. ANOVA showed a significant difference from control: *(P<0.05), ** (P<0.01), *** (P<0.001). **(B)** HepG2 cells were synchronized with serum free media for 48 h and treated with compound **6f** inhibitor at 0, 10 and 20 μM concentrations. Cell cycle progression was measured at 12 h and 24 h. Treated cells were fixed in 70% ethanol, stained with PI and subjected to flow cytometry to measure the % of cell population in different stages of cell cycle, and presented as Bar graph. Data were analyzed by ANOVA and reported as mean ± standard error (SE) of the percentage of the cell population. A significant difference from control was observed by ANOVA: *(P<0.05), ** (P<0.01), # (P<0.001). **(C)** Representative image showing expression level of proteins involved in DNA damage, apoptosis and proliferation measured by Western blot.

3.7. Compound 6f reduces the migration ability of cancer cells

To evaluate the wound healing ability of cancer cells, HepG2 cells were treated with the hLig1 inhibitor at 0, 10 and 20 μM concentrations. Wound healing in control cells without drug treatment was 21.0% and 32.0% at 12 and 18 hours respectively. This was reduced to 11.2% and 16.4% at 12 h and 18 h respectively after treatment with compound **6f** at 10 μM concentration. This was further reduced to 7.5% and 5.5% at 12 h and 18 h respectively using 20 μM concentration. Data was analyzed by ANOVA and reported as the mean ± standard error (SE) of the % wound closure. A significant difference from control was confirmed by ANOVA: *(P<0.05), **(P<0.01), $^{\#}$(P<0.001).

This suggests that compound **6f** reduces the migration ability of HepG2 cells significantly, compared to control (Fig. 7). Hence, this data demonstrates the anti-metastatic activity of this hLig1 inhibitor in hepatic cancer cell line.

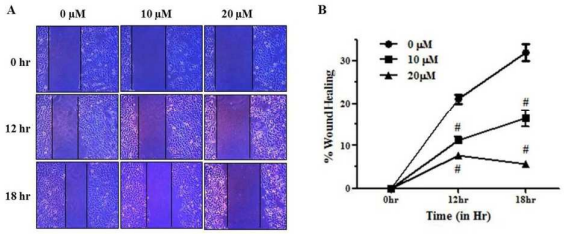

Fig. 7. Compound **6f** reduces the wound healing ability of cancer cells. **(A)** HepG2 cells were grown to confluence in 6 well plates and a scratch (wound) was made by dragging a sterile 200 μL tip uniformly for all the wells. The cells were then treated with compound **6f** at different concentrations (0, 10 and 20 μM) and the ability of cells to repopulate the wound was observed. Images were captured by light microscopy at indicated time points after treatment. Compound **6f** reduced the wound healing ability at 12 h and 18 h compared to control. **(B)** Percentage of wound healing in HepG2 cells were measured after treatment with various concentrations of compound **6f** at indicated time points and presented as line graphs.

View Article Online
DOI: 10.1039/C6MD00447D

3.8. Compound 6f induces cell death in combination with doxorubicin

We also performed a combination study with doxorubicin, a known DNA damaging agent to provide more evidence of on target activity of hLig1 inhibition. Our data shows that compound **6f** has an additive effect with doxorubicin on inducing cell death. In the presence of sub lethal concentration of doxorubicin (0.625 µM) and compound **6f** (5 µM), we observed a significant increase in the cell death compared to compound **6f** or doxorubicin alone (Fig 8). These results confirmed that compound **6f** has the desired effect of targeting the DNA repair machinery by inhibiting the hLig1 enzyme.

3.8. Preliminary *in-vitro* pharmacokinetic properties of compound 6f

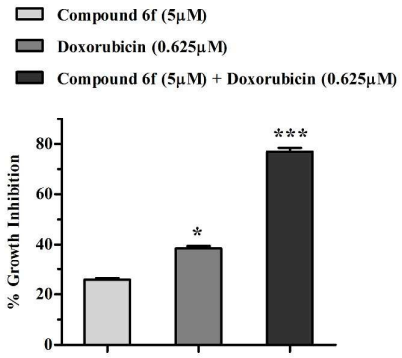

Fig. 8. Combinatorial effect of compound 6f and doxorubicin. HepG2 cells were treated with either compound **6f** (5 µM), or doxorubicin (0.625 µM), or a combination of compound **6f** (5 µM) +doxorubicin (0.625 µM) for 48 h and then subjected to MTT assay. Percentage cell death was calculated and presented as bar graphs. Statistical significance was analysed by ANOVA and reported as mean ± standard error (SE) of the percentage of cell death. ANOVA showed a significant difference from compound **6f**: *(P<0.05), ** (P<0.01), *** (P<0.001).

Encouraged by the interesting results of above experiments we set out to investigate the *in-vitro* pharmacokinetic properties and metabolic stability of synthesised compounds. It is imperative for a new class of molecule to have good ADME properties to pursue it further as a lead molecule. As we were intended to develop orally active drug-like molecules, aqueous solubility is the major factor affecting the oral bioavailability of drugs. The solubility of compound **6f** was found to be 30 µm in triple distilled water (TDW). Subsequently, oral drug delivery potential depends on the stability of drug in the gastrointestinal tract (GIT). Poor stability may affect the absorption of the drug from the GIT and ultimately leads to poor ADME properties. Compound **6f** found stable in the simulated gastric fluid (SGF) and simulated intestinal fluid (SIF) (Fig. 9C) media and these results can favour the good ADME properties. Metabolic stability study is helpful in the designing drug with favourable pharmacokinetic properties. Hence, metabolic stability was assessed by *in-vitro* hamster liver microsomal (HLM) assay using an LC-MS/MS method (Fig. 9A and 9B). The compound **6f** metabolic stability at 1 µm was evaluated in pooled HLM. As shown in data presented in Fig. 9D, compound **6f** was degraded in HLM, with only 12.89 % of the original amount left after 60 min incubation. The calculated *in-vitro* half-life for compound **6f** was 20.82 ± 3.42 min and derived intrinsic clearance (CL_i) was 0.03329 ± 0.0053 mL/min*mg of microsomal protein in pooled HLM. Moreover, it was found stable in the control reactions suggested that cytochrome enzyme plays a major role in the metabolism. Moderate metabolic stability could be helpful for the further advancement of the drug moiety. Plasma protein binding has influence on clearance and distribution indicative of unbound drug, which reflects the pharmacodynamically active drug. Compound **6f** binding with hamster plasma was 99.02 ± 0.04% at the conc. of 10 µm. High plasma protein binding was may be

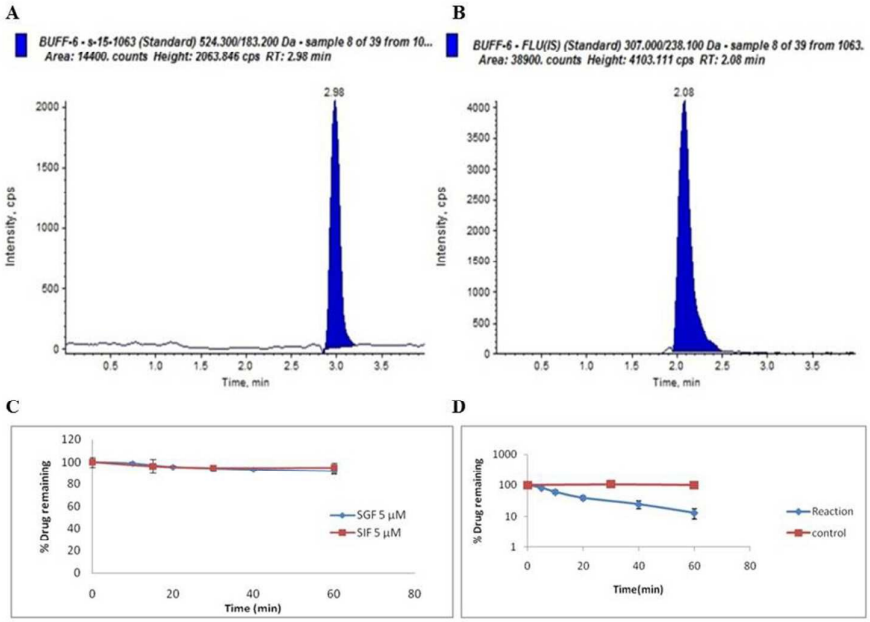

Fig. 9. Representative LC-MS/MS chromatograms of (**A**) compound **6f** (**B**) fluconazole as internal standard (**C**) Stability of the compound **6f** in the SGF and SIF (**D**) Time-dependent metabolic depletion of compound **6f** in Hamster liver microsomes (HLM).

View Article Online
DOI: 10.1039/C6MD00447D

due to the acidic behaviour of the drug.

4. Conclusion

There is a growing interest in testing DNA replication and repair enzymes as appropriate and effective targets for cancer therapy. In the present study, we screened the small molecule inhibitors that can block the hLig1 activity. Using *in-vitro* and *in-silico* approaches, we identified compound **6f** as hLig1 inhibitor that has the ability to target and inhibit the sealing of Okazaki fragments during DNA replication. Our *in-silico* results demonstrate that the inhibitor interacts with the DBD of hLig1 and interacts with key residues involved in DNA binding. This was confirmed by gel shift, fluorescence quenching, and CD spectroscopic analysis.

In the presence of hLig1 inhibitors, the DNA-binding residues are occupied and results in the accumulation of nicks produced during DNA replication. Hence, inhibition of hLig1 would cause hypersensitivity to DNA damaging agents and cell death. This was observed by us in combination drug experiments performed with sub-lethal doses of doxorubicin (a known DNA damaging agent) and **6f** where we observed that sensitivity of HepG2 cells to compound **6f** increased significantly in the presence of doxorubicin. Therefore, compound **6f** interrupts hLig1 mediated nick sealing in DNA of cancer cells, which causes accumulation of DNA strand breaks during replication, results in induction of p53 mediated apoptotic cell death pathway observed in our experiments. We have also confirmed the anti-metastatic property of the identified hLig1 inhibitor. Our results show that compound **6f** reduced the wound healing ability of HepG2 cells in a time and concentration-dependent manner and shows that ligase inhibitors may be active against hepatic cancer cells. Hence, these findings support previous reports that ligase inhibitors have anticancer properties and therefore DNA ligases should be looked at as future therapeutic targets for cancer.

5. Experimental section

5.1. Analysis and instruments

All reagents were commercial and were used without further purification. Chromatography was carried on silica gel (60-120 and 100-200 mesh). All reactions were monitored by thin-layer chromatography (TLC), silica gel plates with fluorescence F254 were used. Melting points were taken in open capillaries on Stuart SMP30 melting point apparatus and are presented uncorrected. Infrared spectra were recorded on a Perkin-Elmer FT-IR RXI spectrophotometer. ^{1}H NMR and ^{13}C NMR spectra were recorded using Bruker Supercon Magnet DRX-300 spectrometer (operating at 300 MHz, 400 MHz, 500 MHz for ^{1}H and 100 MHz for ^{13}C) using $CDCl_3$ and DMSO-d_6 as solvent and tetramethylsilane (TMS) as an internal standard. Chemical shifts are reported in parts per million and multiplicity(s = singlet, brs = broad singlet, d = doublet, brd = broad doublet, dd = double doublet, t = triplet, q = quartet, m = multiplet). Electrospray ionization mass spectra (ESIMS) were recorded on Thermo Lcq Advantage Max-IT. High-resolution mass spectra (HRMS) were recorded on 6520 Agilent Q-Tof LC-MS/MS (Accurate mass).

5.1.1. Representative procedure for the synthesis of compounds 2a-b:

2-methyl/2-*tert*-butyl phenol (1.0 equiv) and hexamethylenetetramine (1.2 equiv) were dissolved in trifluoroacetic acid (25 mL) and the solution was heated at 120 °C for 6-8 h. After cooling to room temperature 10% aq. H_2SO_4 (40 mL) was added and again the temperature was maintained at 90 °C for 4 h. The solution was neutralized with $NaHCO_3$ and extracted with EtOAc. The combined organic layers were dried over Na_2SO_4, filtered, and concentrated to dryness under reduced pressure. The crude products were purified by silica gel column chromatography (60-120 mesh) to afford required compounds (**2a**-**b**).

4-Hydroxy-5-methylisophthalaldehyde (2a). White solid; yield: 54%; mp 125-127 °C; IR (KBr): 3228, 3049, 1719, 1628, 1592, 1208 cm-1; 1H NMR ($CDCl_3$, 300 MHz): δ 11.83 (s, 1H), 9.99 (s, 1H), 9.91 (s, 1H), 7.98 (s, 1H), 7.31 (s, 1H), 2.33 (s, 3H); 13C NMR ($CDCl_3$, 75 MHz): 196.4, 189.7, 164.9, 137.1, 134.7, 128.8, 128.5, 119.7, 15.1; ESI-MS (m/z): 165 $(M+H)^+$.

5-*tert*-butyl-4-hydroxyisophthalaldehyde (2b). Oily, Yield 60%, IR (neat): 3261, 2862, 1711, 1614, 1008 cm^{-1}; ^{1}H NMR ($CDCl_3$, 300 MHz): δ 12.39 (s,1H), 9.99 (s,1H), 9.93 (s,1H), 8.07 (d, *J* = 1.8 Hz, 1H), 7.99 (d, *J* = 2.0 Hz, 1H), 1.46 (s, 9H); ^{13}C NMR ($CDCl_3$, 100 MHz): 196.9, 190.0, 166.1, 140.0, 135.4, 133.9, 128.6, 120.4, 35.2, 29.1; ESI-MS (m/z): 207 $(M+H)^+$.

5.1.2. Representative procedure for the synthesis of compounds 3a-c

To a solution of 4-hydroxy-isophthalaldehyde derivatives (**2a**-**b**) (1.0 equiv) in acetic acid, ethylacetoacetate (1.0 equiv) and urea/thiourea (1.5 equiv) were added. The reaction mixture was heated at 90 °C for 1 h. After completion of reaction (monitored by TLC), the reaction mixture was diluted with cold water and extracted with 3x20 mL of ethyl acetate. The combined organic layers were dried over anhydrous Na_2SO_4 and concentrated under reduced pressure. Thus obtained crude product was purified by column chromatography on 100-200 silica gel, to get compound **3a**-**c** in good yield.

ethyl 4-(3-formyl-4-hydroxy-5-methylphenyl)-6-methyl-2-oxo-1,2,3,4-tetrahydropyrimidine-5-carboxylate (3a). White solid, Yield 72%, mp 238-240 °C; IR (neat): 3508, 3022, 2912, 1711, 1624 cm-1; 1H NMR (500 MHz, $CDCl_3$) δ 11.25 (s, 1H), 9.85 (s, 1H), 7.35 (s, 1H), 7.32 (d, J = 2.1 Hz, 1H), 7.10 (s, 1H), 5.47 (s, 1H), 5.39 (d, J = 2.6 Hz, 1H), 4.12 – 4.07 (m, 2H), 2.37 (s, 3H), 2.25 (s, 3H), 1.20 (t, J = 7.1 Hz, 3H); 13C NMR (100 MHz, $CDCl_3$) δ 196.7, 159.9, 136.4, 135.1, 129.3, 127.8, 119.8, 60.4, 55.3, 19.1, 15.3, 14.4; ESI-MS: (m/z): 319.1 $(M+H)^+$.

ethyl 4-(3-(tert-butyl)-5-formyl-4-hydroxyphenyl)-6-methyl-2-oxo-1,2,3,4-tetrahydropyrimidine-5-carboxylate (3b). Yellow solid, Yield 70%, mp 218-220 °C; IR (neat): 3528, 3014, 2857, 1728, 1611 cm^{-1}; ^{1}H NMR (400 MHz, $CDCl_3$) δ 11.77 (s, 1H), 9.83 (s, 1H), 8.18 (s, 1H), 7.47 (d, *J* = 2.1 Hz, 1H), 7.32 (d, *J* = 2.2 Hz, 1H), 5.93 (s, 1H), 5.40 (d, *J* = 2.1 Hz, 1H), 4.09 (q, *J* = 7.1 Hz, 2H), 2.36 (s, 3H), 1.39 (s, 9H), 1.17 (d, *J* = 7.1 Hz, 3H).; ^{13}C NMR (100 MHz, $CDCl_3$) δ 197.1, 165.7, 161.0,

View Article Online
DOI: 10.1039/C6MD00447D

153.7, 146.6, 138.9, 134.8, 132.9, 129.6, 120.5, 101.4, 60.3, 55.1, 34.9, 29.2, 18.7, 14.3; ESI-MS: (m/z): 361.2 $(M+H)^+$.

ethyl 4-(3-(tert-butyl)-5-formyl-4-hydroxyphenyl)-6-methyl-2-thioxo-1,2,3,4-tetrahydropyrimidine-5-carboxylate (3c). Yellow solid, Yield 62%, mp 251-253 °C; IR (neat): 3425, 3041, 2814, 1707, 1610 cm^{-1}; ^1H NMR (400 MHz, $CDCl_3$) δ 11.81 (s, 1H), 9.84 (s, 1H), 7.91 (s, 1H), 7.44 (d, *J* = 2.2 Hz, 1H), 7.38 (s, 1H), 7.30 (d, *J* = 2.2 Hz, 1H), 5.39 (d, *J* = 2.8 Hz, 1H), 4.15 – 4.09 (m, 2H), 2.38 (s, 3H), 1.39 (s, 9H), 1.19 (t, *J* = 7.1 Hz, 3H).; ^{13}C NMR (100 MHz, $CDCl_3$) δ 197.1, 174.6, 165.3, 161.3, 143.1, 139.1, 133.6, 132.9, 129.9, 120.6, 103.0, 60.7, 55.6, 35.0, 29.2, 18.5, 14.3; ESI-MS: (m/z): 377.2 $(M+H)^+$.

5.1.3. Representative procedure for the synthesis of compounds 5a-e

Different substituted isocyanates were added drop wise to an ice-cold stirred solution of hydrazine hydrate in DCM over a period of 30 min. After the completion of addition reaction allowed to warm to the room temperature and allowed to stir for about 4 h. After the completion of time, white solid separated out which was filtered and recrystalised from ethanol to get desired product in good to excellent yield. All synthesized N-phenylhydrazinecarbothioamide were conformed from literature reports.[21]

5.1.4. Representative procedure for the synthesis of compounds 5f-h

To a solution of aniline derivatives in DMF solvent, NaOH and carbondisulphide were added. The mixture was stirred at 20-25 °C for 1h. To the stirred mixture, hydrazine hydrate was added and stirring continued at 80 °C for 1h. On addition of water, a solid separated out which was recrystallized from absolute ethanol. All the derivatives were confirmed by reported data.[22]

5.1.5. Representative procedure for the synthesis of compounds 6a-q

A mixture of dihydropyrimidinone derivatives (**3a**-**c**, 1 equiv) and N-phenylhydrazinecarbothioamide derivatives (**5a**-**h**, 1 equiv) were dissolved in ethanol and stirred at room temperature till the reactants are consumed. After the completion of reaction (as monitored by TLC), the excess solvent was evaporated under reduced pressure. The resultant residue was purified by flash chromatography ($MeOH/CHCl_3$ as the eluent) to afford target hybrid compounds **6a-q**.

ethyl (E)-4-(3-(tert-butyl)-5-((2-((4-chlorophenyl)carbamoyl)hydrazono)methyl)-4-hydroxyphenyl)-6-methyl-2-thioxo-1,2,3,4-tetrahydropyrimidine-5-carboxylate (**6a**). White solid, Yield 91%, mp 249-251 °C; IR (neat): 3650, 3429, 2968, 1745, 1670, 742 cm^{-1}; ^1H NMR (400 MHz, DMSO-d_6) δ 11.38 (s, 1H), 10.50 (s, 1H), 10.31 (s, 1H), 9.60 (s, 1H), 9.25 (s, 1H), 8.20 (s, 1H), 7.56 (d, *J* = 8.9 Hz, 2H), 7.34 (d, *J* = 8.8 Hz, 2H), 7.18 (s, 1H), 7.01 (d, *J* = 1.8 Hz, 1H), 5.13 (d, *J* = 3.3 Hz, 1H), 4.03 (q, *J* = 7.0 Hz, 2H), 2.29 (s, 3H), 1.38 (s, 9H), 1.11 (t, *J* = 7.1 Hz, 3H); ^{13}C NMR ($CDCl_3$, 100 MHz): 174.6, 165.6, 155.6, 152.4, 146.2, 145.2, 138.7, 136.9, 134.5, 128.9, 126.9, 126.7, 126.5, 121.3, 118.6, 101.4, 60.1, 54.1, 34.9, 29.6, 17.6, 14.5; HRMS (ESI) calcd for $C_{26}H_{30}ClN_5O_4S$ $[M + H]^+$ 544.1780, found 544.1785.

ethyl (E)-4-(3-(tert-butyl)-4-hydroxy-5-((2-(p-tolylcarbamothioyl)hydrazono)methyl)phenyl)-6-methyl-2-thioxo-1,2,3,4-tetrahydropyrimidine-5-carboxylate (6b). Yellow solid, Yield 82%, mp 271-273 °C; IR (neat): 3643, 3415, 2927, 1752, 1645, 723 cm^{-1}; ^1H NMR (400 MHz, DMSO-d_6) δ 11.58 (s, 1H), 10.35 (s, 1H), 10.11 (s, 1H), 9.62 (s, 1H), 8.36 (s, 1H), 7.36 (d, *J* = 6.9 Hz, 2H), 7.23 (s, 1H), 7.18 (d, *J* = 6.9 Hz, 2H), 7.05 (s, 1H), 5.15 (s, 1H), 4.04 (q, *J* = 7.2 Hz, 2H), 2.32 (s, 3H), 2.29 (s, 3H), 1.38 (s, 9H), 1.14 (t, *J* = 6.9 Hz, 3H); ^{13}C NMR (DMSO-d_6, 100 MHz): 174.6, 165.7, 155.3, 147.6, 145.1, 137.4, 136.8, 135.1, 129.8, 129.2, 127.4, 127.3, 125.9, 118.6, 117.4, 101.5, 60.1, 53.9, 34.8, 29.5, 20.9, 17.5, 14.4; HRMS (ESI) calcd for $C_{27}H_{33}N_5O_3S_2$ $[M + H]_+$ 540.2098, found 540.2084.

ethyl (*E*)-4-(3-(*tert*-butyl)-4-hydroxy-5-((2-(phenylcarbamothioyl)hydrazono)methyl)phenyl)-6-methyl-2-thioxo-1,2,3,4-tetrahydropyrimidine-5-carboxylate (6c). White solid, Yield 83%, mp 268-270 °C; IR (neat): 3615, 3455, 2932, 1722, 1645, 746 cm^{-1}; ^1H NMR (400 MHz, DMSO-d_6) δ 11.64 (s, 1H), 10.35 (s, 1H), 10.18 (s, 1H), 9.63 (s, 1H), 8.37 (s, 1H), 7.51 (d, *J* = 6.6 Hz, 2H), 7.38 (bs, 2H), 7.23 (bs, 2H), 7.06 (s, 1H), 5.15 (s, 1H), 4.03 (q, *J* = 7.2 Hz, 2H), 2.30 (s, 3H), 1.39 (s, 9H), 1.14 (t, *J* = 6.9 Hz, 3H); ^{13}C NMR (DMSO-d_6, 100 MHz): 174.8, 165.6, 155.3, 147.9, 145.3, 139.7, 137.4, 134.9, 128.7, 127.5, 126.0, 125.8, 118.7, 101.5, 60.1, 54.0, 35.0, 29.7, 17.6, 14.5; HRMS (ESI) calcd for $C_{26}H_{31}N_5O_3S_2$ $[M + H]^+$ 526.1941, found 526.1931.

ethyl (*E*)-4-(3-(*tert*-butyl)-5-((2-((4-chlorophenyl)carbamothioyl)hydrazono)methyl)-4-hydroxyphenyl)-6-methyl-2-thioxo-1,2,3,4-tetrahydropyrimidine-5-carboxylate (6d). Pale yellow solid, Yield 88%, mp 271-273 °C; IR (neat): 3674, 3420, 2965, 1725, 1611, 742 cm^{-1}; ^1H NMR (400 MHz, DMSO-d_6) δ 11.73 (s, 1H), 10.35 (s, 1H), 10.22 (s, 1H), 9.62 (s, 1H), 8.37 (s, 1H), 7.55 (d, *J* = 7.4 Hz, 2H), 7.43 (d, *J* = 7.1 Hz, 2H), 7.24 (s, 1H), 7.06 (s, 1H), 5.15 (s, 1H), 4.03 (q, *J* = 7.0 Hz, 2H), 2.29 (s, 3H), 1.38 (s, 9H), 1.13 (t, *J* = 7.0 Hz, 3H); ^{13}C NMR (DMSO-d_6, 100 MHz): 174.8, 165.7, 155.3, 148.2, 145.3, 138.7, 137.4, 135.0, 129.8, 128.6, 127.6, 118.6, 101.4, 60.1, 54.0, 35.0, 29.7, 17.6, 14.5; HRMS (ESI) calcd for $C_{26}H_{30}ClN_5O_3S_2$ $[M + H]^+$ 560.1551, found 560.1549

ethyl (E)-4-(3-(tert-butyl)-4-hydroxy-5-((2-(phenylcarbamoyl)hydrazono)methyl)phenyl)-6-methyl-2-thioxo-1,2,3,4-tetrahydropyrimidine-5-carboxylate (6e). White solid, Yield 78%, mp 235-237 °C; IR (neat): 3641, 3471, 2914, 1774, 1621, 714 cm^{-1}; ^1H NMR (400 MHz, DMSO-d_6) δ 11.50 (s, 1H), 10.44 (s, 1H), 10.32 (s, 1H), 9.61 (s, 1H), 9.09 (s, 1H), 8.21 (s, 1H), 7.53 (d, *J* = 7.6 Hz, 2H), 7.30 (t, *J* = 7.9 Hz, 2H), 7.19 (d, *J* = 1.9 Hz, 1H), 7.03-7.01 (m, 2H), 5.14 (d, *J* = 3.5 Hz, 1H), 4.08-3.99 (m, 2H), 2.30 (s, 3H), 1.39 (s, 9H), 1.13 (t, *J* = 7.1 Hz, 3H); ^{13}C NMR (DMSO-d_6, 100 MHz): 174.7, 165.7, 155.7, 152.5, 145.9, 145.2, 139.7, 136.9, 134.5, 129.1, 126.8, 126.6, 122.9, 119.7, 118.7, 101.4, 60.0, 54.1, 34.9, 29.7, 17.6, 14.5; HRMS (ESI) calcd for $C_{26}H_{31}N_5O_4S$ $[M + H]^+$ 510.2170, found 510.2170.

ethyl (E)-4-(3-(tert-butyl)-4-hydroxy-5-((2-((3-methoxyphenyl)carbamoyl)hydrazono)methyl)phenyl)-6-methyl-2-oxo-1,2,3,4-tetrahydropyrimidine-5-carboxylate

View Article Online
DOI: 10.1039/C6MD00447D

(6f). Yellow solid, Yield 81%, mp 239-241 °C; IR (neat): 3611, 3389, 2937, 1730, 1618, 712 cm^{-1}; ^1H NMR (400 MHz, DMSO-d_6) δ 11.49 (s, 1H), 10.39 (s, 1H), 9.17 (s, 1H), 9.08 (s, 1H), 8.21 (s, 1H), 7.68 (s, 1H), 7.24 (t, *J* = 2.1 Hz, 1H), 7.22 – 7.18 (m, 2H), 7.06 – 7.03 (m, 2H), 6.61 – 6.58 (m, 1H), 5.11 (d, *J* = 3.1 Hz, 1H), 4.03 – 3.97 (m, 2H), 3.75 (s, 3H), 2.26 (s, 3H), 1.39 (s, 9H), 1.12 (t, *J* = 7.1 Hz, 3H); ^{13}C NMR (DMSO-d_6, 100 MHz): 165.4, 159.6, 155.5, 152.2, 151.9, 148.0, 145.7, 140.5, 136.2, 135.3, 129.4, 126.2, 126.0, 118.1, 111.4, 107.8, 104.8, 99.5, 59.1, 54.9, 53.6, 34.4, 29.2, 17.7, 14.1; HRMS (ESI) calcd for $C_{27}H_{33}N_5O_6$ $[M + H]^+$ 524.2504, found 524.2472.

ethyl (*E*)-4-(3-(tert-butyl)-5-((2-((4-fluorophenyl)carbamoyl)hydrazono)methyl)-4-hydroxyphenyl)-6-methyl-2-*oxo*-1,2,3,4-tetrahydropyrimidine-5-carboxylate (6g). White solid , Yield 84%, mp 242-244 °C; IR (neat): 3677, 3406, 2936, 1744, 1666, 730 cm^{-1}; ^1H NMR (400 MHz, DMSO-d_6) δ 11.80 (s, 1H), 9.97 (s, 1H), 9.23 (s, 1H), 8.83 (s, 1H), 8.00 (s, 1H), 7.74 (s, 1H), 7.54 – 7.50 (m, 3H), 7.44 (d, *J* = 2.2 Hz, 1H), 7.09 (t, *J* = 8.9 Hz, 2H), 5.16 (d, *J* = 3.2 Hz, 1H), 4.00 (q, *J* = 6.8 Hz, 2H), 2.27 (s, 3H), 1.37 (s, 9H), 1.10 (t, *J* = 7.1 Hz, 3H); ^{13}C NMR (DMSO-d_6, 100 MHz): 199.0, 165.7, 159.6, 159.0, 156.7, 152.4, 149.1, 137.6, 136.6, 133.1, 129.6, 120.9, 120.8, 115.6, 115.4, 99.4, 59.7, 54.0, 34.8, 29.5, 18.3, 14.6; HRMS (ESI) calcd for $C_{26}H_{30}FN_5O_5$ $[M + H]^+$ 512.2304, found 512.2311

ethyl (*E*)-4-(3-((2-((4-bromophenyl)carbamoyl)hydrazono)methyl)-5-(*tert*-butyl)-4-hydroxyphenyl)-6-methyl-2-*oxo*-1,2,3,4-tetrahydropyrimidine-5-carboxylate (6h). White solid, Yield 78%, mp 277-279 °C; IR (neat): 3701, 3478, 2947, 1695, 1580, 789 cm^{-1}; ^1H NMR (400 MHz, DMSO-d_6) δ 11.32 (s, 1H), 10.50 (s, 1H), 9.26 (s, 1H), 9.17 (s, 1H), 8.21 (s, 1H), 7.68 (s, 1H), 7.53 (d, *J* = 9.0 Hz, 2H), 7.47 (d, *J* = 8.9 Hz, 2H), 7.20 (d, *J* = 1.7 Hz, 1H), 7.03 (d, *J* = 1.7 Hz, 1H), 5.11 (d, *J* = 3.0 Hz, 1H), 4.02 - 3.98 (m, 2H), 2.26 (s, 3H), 1.39 (s, 9H), 1.12 (t, *J* = 7.1 Hz, 3H); ^{13}C NMR (100 MHz, DMSO-d_6): 165.8, 155.4, 152.6, 152.4, 148.5, 146.4, 139.2, 136.6, 135.8, 131.8, 126.7, 126.6, 121.5, 118.4, 114.3, 99.9, 59.6, 54.1, 34.9, 29.7, 18.2, 14.6; HRMS (ESI) calcd for $C_{26}H_{30}BrN_5O_5$ $[M + H]^+$ 572.1503, found 572.1527.

ethyl (E)-4-(3-(tert-butyl)-4-hydroxy-5-((2-(phenylcarbamothioyl)hydrazono)methyl)phenyl)-6-methyl-2-oxo-1,2,3,4-tetrahydropyrimidine-5-carboxylate (6i). White solid, Yield 81%, mp 237-239 °C; IR (neat): 3688, 3512, 2978, 1745, 1692, 689 cm^{-1}; ^1H NMR (500 MHz, DMSO-d_6) δ 11.62 (s, 1H), 10.18 (s, 1H), 9.20 (s, 1H), 8.36 (s, 1H), 7.71 (s, 1H), 7.51 (d, *J* = 7.7 Hz, 2H), 7.38 (t, *J* = 7.5 Hz, 2H), 7.24 (s, 1H), 7.21 (t, *J* = 7.2 Hz, 1H), 7.06 (s, 1H), 5.12 (d, *J* = 3.0 Hz, 1H), 4.04 – 3.99 (m, 2H), 2.25 (s, 3H), 1.38 (s, 9H), 1.12 (t, *J* = 6.8 Hz, 3H); ^{13}C NMR (100 MHz, DMSO-d_6): 165.9, 155.0, 152.7, 148.6, 148.1, 139.7, 137.1, 136.2, 128.7, 127.5, 127.4, 126.0, 125.8, 118.5, 99.9, 59.7, 53.9, 35.0, 29.7, 18.2, 14.6; HRMS (ESI) calcd for $C_{26}H_{31}N_5O_4S$ $[M + H]^+$ 510.2170, found 510.2173.

ethyl (E)-4-(3-(tert-butyl)-5-((2-((4-chlorophenyl)carbamothioyl)hydrazono)methyl)-4-hydroxyphenyl)-6-methyl-2-oxo-1,2,3,4-tetrahydropyrimidine-5-carboxylate (6j). White solid, Yield 79%, mp 213-215 °C; IR (neat): 3704, 3512, 2959, 1733, 1698, 722 cm^{-1}; ^1H NMR (400 MHz, DMSO-d_6) δ 11.70 (s, 1H), 10.23 (s, 1H), 9.20 (s, 1H), 8.36 (s, 1H), 7.71 (s, 1H), 7.55 (d, *J* = 8.8 Hz, 2H), 7.43 (d, *J* = 8.8 Hz, 2H), 7.25 (d, *J* = 1.9 Hz, 1H), 7.06 (d, *J* = 1.9 Hz, 1H), 5.12 (d, *J* = 3.0 Hz, 1H), 4.02 – 3.99 (m, 2H), 2.25 (s, 3H), 1.38 (s, 9H), 1.12 (t, *J* = 7.1 Hz, 3H); ^{13}C NMR (100 MHz, DMSO-d_6): 165.9, 155.1, 152.7, 148.7, 148.5, 138.7, 137.1, 136.2, 129.8, 128.6, 127.6, 118.4, 99.9, 59.7, 53.9, 34.9, 29.7, 18.2, 14.6; HRMS (ESI) calcd for $C_{26}H_{30}ClN_5O_4S$ $[M + H]^+$ 544.1780, found 544.1772.

ethyl (E)-4-(3-(tert-butyl)-4-hydroxy-5-((2-(methylcarbamothioyl)hydrazono)methyl)phenyl)-6-methyl-2-oxo-1,2,3,4-tetrahydropyrimidine-5-carboxylate (6k). White solid, Yield 77%, mp 196-198 °C; IR (neat): 3711, 3431, 2974, 1744, 1632, 752 cm^{-1}; ^1H NMR (400 MHz, DMSO- d_6) δ 11.30 (s, 1H), 9.97 (s, 1H), 9.19 (d, *J* = 1.5 Hz, 1H), 8.46 (d, *J* = 4.4 Hz, 1H), 8.26 (s, 1H), 7.69 (d, *J* = 2.7 Hz, 1H), 7.22 (d, *J* = 2.0 Hz, 1H), 6.99 (d, *J* = 2.1 Hz, 1H), 5.11 (d, *J* = 3.2 Hz, 1H), 4.02 -3.99 (m, 2H), 3.02 (d, *J* = 4.4 Hz, 3H), 2.25 (s, 3H), 1.39 (s, 9H), 1.12 (t, *J* = 7.1 Hz, 3H); ^{13}C NMR (100 MHz, DMSO-d_6): 177.8, 165.8, 154.8, 152.7, 148.6, 147.5, 136.9, 136.2, 127.6, 127.2, 118.3, 99.9, 59.7, 53.9, 34.9, 31.7, 29.7, 18.2, 14.6; HRMS (ESI) calcd for $C_{21}H_{29}N_5O_4S$ $[M + H]^+$ 448.2013, found 448.2046.

ethyl (E)-4-(3-(tert-butyl)-5-((2-carbamoylhydrazono)methyl)-4-hydroxyphenyl)-6-methyl-2-oxo-1,2,3,4-tetrahydropyrimidine-5-carboxylate (6l). White solid, Yield 81%, mp 185-187 °C; IR (neat): 3701, 3445, 2917, 1751, 1674, 756 cm^{-1}; ^1H NMR (400 MHz, DMSO) δ 11.12 (s, 1H), 10.17 (s, 1H), 9.16 (d, *J* = 1.6 Hz, 1H), 8.06 (s, 1H), 7.72 – 7.63 (m, 1H), 7.17 (d, *J* = 2.1 Hz, 1H), 6.96 (d, *J* = 2.1 Hz, 1H), 6.37 (s, 2H), 5.09 (d, *J* = 3.2 Hz, 1H), 4.04 – 3.96 (m, 2H), 2.25 (s, 3H), 1.38 (s, 9H), 1.11 (t, *J* = 7.1 Hz, 3H); ^{13}C NMR (100 MHz, DMSO-d_6): 165.9, 155.9, 155.2, 152.7, 148.5, 144.7, 136.5, 135.7, 126.4, 126.3, 118.6, 100.0, 59.6, 54.0, 49.0, 34.9, 29.7, 18.2, 14.6; HRMS (ESI) calcd for $C_{20}H_{27}N_5O_5$ $[M + H]^+$ 418.2085, found 418.2087.

ethyl (E)-4-(3-(tert-butyl)-5-((2-carbamothioylhydrazono)methyl)-4-hydroxyphenyl)-6-methyl-2-oxo-1,2,3,4-tetrahydropyrimidine-5-carboxylate (6m). White solid, yield: 79%; mp 225-227 °C; IR(neat): 3709, 3455, 2935, 1745, 1674, 711 cm^{-1}; ^1H NMR (DMSO-d_6, 400 MHz): *δ* 11.30 (s, 1H), 9.90 (s, 1H), 9.19 (d, *J* =1.6 Hz, 1H), 8.24 (s, 1H), 8.04 (bs, 2H), 7.69 (m, 3H), 7.22 (d, *J* =2.12 Hz, 1H), 7.00 (d, *J* =2.4 Hz, 3H), 5.11 (d, *J* =3.2 Hz, 1H), 4.02-3.99 (m, 2H), 2.24 (s, 3H), 1.37(s, 9H), 1.12 (t, *J* = 7.1 Hz, 3H), ^{13}C NMR (DMSO-d_6, 75 MHz): *δ* 165.8, 155.0, 152.6, 148.5, 147.6, 136.9, 136.1, 127.4, 127.2, 118.3, 99.9, 79.6, 59.6, 53.9, 40.5, 40.3, 40.1, 39.9, 39.7, 39.5, 39.3, 34.9, 29.6, 18.2, 14.6; HRMS (ESI) calcd for $C_{20}H_{27}N_5O_4S$ $[M + H]^+$ 434.1857, found 434.1864.

ethyl (E)-4-(3-((2-((4-chlorophenyl)carbamoyl)hydrazono)methyl)-4-hydroxy-5-methylphenyl)-6-methyl-2-thioxo-1,2,3,4-tetrahydropyrimidine-5-carboxylate (6n). White solid, Yield 85%, mp 241-243 °C; IR (neat): 3688, 3478, 2944, 1741, 1625, 742 cm^{-1}; ^1H NMR (400 MHz, DMSO-d_6) δ 10.61 (s, 1H), 10.29 (s, 1H), 9.59 (s, 1H), 9.14 (s, 1H), 8.21 (s, 1H), 7.60 (d, *J* = 8.9 Hz, 2H), 7.35 (d, *J* = 8.8 Hz, 2H), 7.14 (d, *J* = 1.8 Hz, 1H), 7.01 (d, *J* = 1.7 Hz, 1H), 5.13 (d, *J* = 3.5 Hz, 1H), 4.04-4.01 (m, 2H), 2.30 (s,

View Article Online
DOI: 10.1039/C6MD00447D

3H), 2.19 (s, 3H), 1.12 (t, *J* = 7.1 Hz, 3H); ^{13}C NMR (100 MHz, DMSO-d_6): 174.3, 165.9, 154.6, 152.9, 145.2, 138.1, 134.8, 130.5, 129.0, 127.0, 126.0, 125.6, 121.6, 118.6, 101.4, 60.3, 54.0, 17.6, 16.3, 14.3; HRMS (ESI) calcd for $C_{23}H_{24}ClN_5O_4S$ [M + H]$^+$ 502.1310, found 502.1310.

ethyl (E)-4-(4-hydroxy-3-methyl-5-((2-(methylcarbamothioyl)hydrazono)methyl)phenyl)-6-methyl-2-oxo-1,2,3,4-tetrahydropyrimidine-5-carboxylate (6o). White solid, Yield 80%, mp 249-251 °C; IR (neat): 3720, 3441, 2952, 1721, 1645, 702 cm^{-1}; ^{1}H NMR (400 MHz, DMSO-d_6) δ 11.36 (s, 1H), 9.45 (s, 1H), 9.14 (d, *J* = 1.6 Hz, 1H), 8.41 (d, *J* = 4.4 Hz, 1H), 8.29 (s, 1H), 7.65 – 7.64 (m, 1H), 7.12 (d, *J* = 2.0 Hz, 1H), 7.03 (d, *J* = 1.7 Hz, 1H), 5.10 (d, *J* = 3.1 Hz, 1H), 4.03 – 3.94 (m, 2H), 3.01 (d, *J* = 4.5 Hz, 3H), 2.25 (s, 3H), 2.19 (s, 3H), 1.12 (t, *J* = 7.1 Hz, 3H); ^{13}C NMR (100 MHz, DMSO-d_6): 177.4, 165.4, 153.4, 152.0, 148.1, 144.8, 136.1, 130.1, 126.0, 125.2, 117.8, 99.3, 59.2, 53.5, 31.1, 17.8, 16.1, 14.1; HRMS (ESI) calcd for $C_{18}H_{23}N_5O_4S$ [M + H]$^+$ 406.1544, found 406.1529.

ethyl (E)-4-(3-((2-carbamoylhydrazono)methyl)-4-hydroxy-5-methylphenyl)-6-methyl-2-oxo-1,2,3,4-tetrahydropyrimidine-5-carboxylate (6p). White solid, Yield 77%, mp 266-268 °C; IR (neat): 3678, 3429, 2911, 1745, 1654, 718 cm^{-1}; ^{1}H NMR (400 MHz, DMSO-d_6) δ 10.19 (s, 1H), 9.13 (d, *J* = 1.6 Hz, 1H), 8.07 (s, 1H), 7.64 – 7.62 (m, 1H), 7.05 (d, *J* = 2.0 Hz, 1H), 6.99 (d, *J* = 1.7 Hz, 1H), 6.38 (s, 2H), 5.08 (d, *J* = 3.1 Hz, 1H), 4.04-3.95 (m, 2H), 2.25 (s, 3H), 2.17 (s, 3H), 1.11 (t, *J* = 7.1 Hz, 3H); ^{13}C NMR (100 MHz, DMSO-d_6): 165.9, 156.3, 154.0, 152.6, 148.5, 142.8, 136.2, 129.9, 125.5, 125.3, 118.6, 99.8, 59.6, 53.9, 18.3, 16.4, 14.6; HRMS (ESI) calcd for $C_{17}H_{21}N_5O_5$ [M + H]$^+$ 376.1615, found 376.1604.

ethyl (E)-4-(3-((2-carbamothioylhydrazono)methyl)-4-hydroxy-5-methylphenyl)-6-methyl-2-oxo-1,2,3,4-tetrahydropyrimidine-5-carboxylate (6q). White solid, Yield 81%, mp 271-273 °C; IR (neat): 3678, 3436, 2944, 1712, 1648, 721 cm^{-1}; ^{1}H NMR (400 MHz, DMSO-d_6) δ 11.34 (s, 1H), 9.34 (s, 1H), 9.13 (s, 1H), 8.29 (s, 1H), 8.17 (s, 1H), 7.90 (s, 1H), 7.63 (s, 1H), 7.16 (s, 1H), 7.02 (s, 1H), 5.08 (d, *J* = 2.3 Hz, 1H), 4.01 – 3.94 (m, 2H), 2.24 (s, 3H), 2.17 (s, 3H), 1.10 (t, *J* = 7.0 Hz, 3H); ^{13}C NMR (100 MHz, DMSO-d_6): 165.4, 153.6, 152.0, 148.1, 144.8, 136.1, 130.2, 125.6, 125.4, 99.3, 59.2, 53.4, 17.8, 16.2, 14.1; HRMS (ESI) calcd for $C_{17}H_{21}N_5O_4S$ [M + H]$^+$ 392.1387, found 392.1364.

5.2. Biological protocols

5.2.1. Purification of hLig1 protein

Human DNA ligase1 protein was over expressed and purified as described earlier.[25] In brief, the pRSF-Duet1-hLig1 plasmid was transformed into BL21(DE3)RP cells. The hLig1 protein was purified by ion exchange chromatography using phosphocellulose column and heparin column, followed by gel filtration chromatography. Protein was dialyzed against storage buffer (25 mM Tris-Cl pH7.5, 150 mM NaCl, 0.1 mM EDTA, 4 mM DTT, protease inhibitors), concentrated, quantified and used for further experiments.

The DBD (hLig1) was expressed and purified same as described previously.[13] *E. coli* BL21(DE3)RP cells were transformed with pET28a-DBD (hLig1) plasmid. Transformed cells were grown in 2XYT media and overexpressed at 16 °C. N-terminally His-tagged DBD was purified over Ni^{2+}-NTA resin (Macharey-Nagel) and further purified by gel filtration chromatography using Superdex 200, 10/300GL column (GE Biosciences) connected to AKTA FPLC (GE Biosciences). Protein was dialyzed against storage buffer (25mM Tris-HCl (pH 7.5), 150 mM NaCl, 2 mM DTT, 10% Glycerol and protease inhibitors). DBD-protein containing fractions were collected, and purity was estimated by 12% SDS-PAGE.

5.2.2. DNA nick joining assay

DNA nick joining assay was performed as discussed previously.[16b] A fluorescently labelled double stranded nicked DNA was used as a substrate for the hLig1 enzyme. DNA substrate was prepared by annealing cyanin3 labelled 27-mer oligo with 52-mer and 25-mer, to form a complementary double stranded nicked DNA. The double-stranded nicked DNA (1 pmol) was incubated with the purified hLig1 (0.2 pmol) using ligation buffer [50 mM Tris-Cl (pH 7.5), 100 mM NaCl, 10 mM $MgCl_2$, 0.25 mg/ml BSA and 500 µM ATP] in the absence or presence of inhibitors at 37 °C for 30 min. stop buffer was added to terminate the ligation reaction. The DNA molecules were separated on a urea gel and bands were visualized by using image quant LAS 4010 (GE Life Sciences).

5.2.3. Circular Dichroism Spectroscopy

To evaluate the binding specificity of compound **6f** to full-length hLig1 and the DBD domain, we have used Far-UV CD spectroscopy. Purified hLig1 and DBD proteins were dialyzed against buffer containing 10 mM Tris-Cl, pH 7.6, 10 mM NaCl, 0.1 mM EDTA, and diluted according to experiments used for spectra acquisition. CD spectra were collected for hLig1 (1.75 µM) and DBD (3.75 µM) in the presence or absence of compound **6f** using a JASCO J-810 spectropolarimeter equipped with Peltier block arrangement for temperature control. The spectra were collected using a quartz cuvette with a path length of 1.0 mm, in the wavelength range of 195–250 nm using a spectral bandwidth of 1 nm and scanning speed 100 nm/min at room temperature. Three independent CD spectra were averaged for each sample and their matched buffer. The mean residual ellipticity (MRE) was calculated and plotted using Graph Pad Prism software.

5.2.4. Cell viability and clonogenic survival assay

Effect of compound **6f** on cell viability was evaluated by MTT assay as described previously.[16] HepG2 cells were seeded out in 96 well plates at a density of 1 x 10^3 cells/mL with 100 µL media (supplemented with 10% FBS) in each well. After 12 hours of incubation, cells were treated with various concentrations of compound **6f** inhibitor (0, 6.25, 12.5, 25.0 and 50 µM) for 48 h. DMSO treated cells were used as a control. For cell viability assays, 10 µL of MTT solution (5 mg/mL) was added to each well and incubated at 37 °C for 4 h. The media was removed and 100 µL DMSO was added to dissolve formazan pellets, and absorbance was measured at a wavelength of 570 nm.

For clonogenic survival assay, HepG2 cells (400 cells/well each) were grown overnight in DMEM culture media supplemented with 10% FBS. Cells were treated with compound **6f** inhibitor molecules at various concentrations (0, 5, 10 and 20 µM) for

View Article Online
DOI: 10.1039/C6MD00447D

48 hr. After that, culture medium was replaced with fresh medium and cells were cultured again for next ten days while changing media every three days. Cells were washed with 1XPBS, stained with 0.5% crystal violet and fixed with 6.0% glutaraldehyde for 30 min at room temperature. Finally, cells were washed with tap water gently to remove the excess stain; plates were air dried, and images were captured.

5.2.5. Flow cytometry analysis of apoptotic cell death and cell cycle progression

Apoptotic cell death was analysed as described previously.[16] Briefly, HepG2 cells were incubated with various concentrations of compound **6f** (0, 5, 10 and 20μM) for 48 h. The cells were harvested, processed and stained with Annexin-V FITC and propidium iodide (PI). After staining, cells were subjected to flow cytometry (BD Biosciences, USA) analysis.

For cell cycle analysis, HepG2 cells were plated out in 6 well plates ($1.5x10^5$ cells/mL) with 2mL media in each well. After 12 hours of incubation, cells were synchronized by using serum free media for 48 h and then treated with compound **6f** at 10 and 20 μM concentrations in complete media. Cells were harvested at various time intervals, washed with ice-cold 1XPBS and permeabilized using ice cold 70% ethanol at -20 °C. The fixed cells were centrifuged, washed and stained with PI (50 μg/mL) containing DNase-free RNase (100 μg/mL). After staining, samples were subjected to flow cytometry (BD Biosciences, USA) analysis.

5.2.6. Preparation cell lysate and western blotting

HepG2 cells were treated with compound **6f** at 10 and 20 μM concentrations. After 48 hr of treatment, cells were harvested and washed with chilled 1xPBS twice. Cells were lysed by sonication in the PBS containing protease inhibitor. The cell lysates were collected after centrifugation of lysed samples at 10,000 rpm for 30 min at 4 °C. Proteins were resolved by SDS-PAGE and transferred to PVDF membrane. The membranes were incubated with desired primary antibodies (PCNA, γ-H2AX, P53) and β-actin was used as a loading control to ensure equal protein loading. Further, membranes were incubated with appropriate HRP-conjugated secondary antibodies and visualised by enhanced chemiluminescence using Image Quant LAS 4010 (GE Life Sciences).

5.2.7. DNA intercalation assay

For the gel-based assay, intercalation ability of hLig1 inhibitor with DNA substrate was evaluated same as discussed earlier.[26] In brief, linearized pUC18 plasmid was incubated with hLig1 inhibitor up to 600 μM concentration for 30 min at 37 °C. Doxorubicin and Ampicillin were used as positive and negative controls respectively. Shift in the plasmid DNA bands were detected and visualized on a 1% agarose gel.

We also performed Ethidium Bromide (EtBr) displacement assay in order to check the DNA intercalation ability of hLig1 inhibitor using fluorescence spectroscopy method. EtBr displacement is detected on the strong loss in fluorescence upon its detachment from DNA.[27] Plasmid DNA (2.5 μg) and EtBr (125 μM) was incubated with different concentrations of inhibitors in a buffer (25 mM Tris-HCl (pH 8.0), 50 mM NaCl and 1 mM EDTA). Change in EtBr fluorescence intensity upon addition of increasing concentrations of compound **6f** was measured at the wavelength 485 nm (excitation) and 612 nm (emission).

5.2.8. Wound healing assay

The wound healing/scratch assay was performed as described previously.[16a] Briefly, HepG2 cells were grown in six-well plates using DMEM culture medium supplemented with 10% FBS. Confluent monolayer cells were wounded by dragging a sterile 200 μL pipette tip and washed with PBS to remove detached cells from the plates. Cells were treated with compound **6f** inhibitor at 0, 10 and 20 μM concentrations. The extent of wound healing (wound closure) was observed by microscopy at 0, 12 and 18 h time points.

5.2.9. Aqueous solubility

Aqueous solubility of compound **6f** was determined by using a Nephelometry assay.[28] compound **6f** stock solution was prepared in DMSO and further diluted to produce a wide range of working stocks. These working stocks were added to the TDW to obtain final concentrations of 1 μM, 3 μM, 10 μM, 30 μM, 100 μM, 300 μM, and 1000 μM by keeping 1% organic content. Then incubation was carried out for 2hr at 37 °C and absorbance was recorded at 620 nm by using nephelometer (BMG LABTECH, Germany).

5.2.10. pH-dependent stability

For the oral route of administration, drug should be stable in the GIT before reaching to the systemic circulation. *In-vitro* SGF – pH 1.2 / SIF pH- 6.8 mimics the GIT conditions. The SGF and SIF were prepared according to USP. Briefly, 5μM compound was incubated in SGF/SIF. At different time intervals (0, 10, 20, 40, 60 min for SGF and 0,15,30,60, 120 min. for SIF) 100 μL of samples were collected and quenched with 300 μL of the ice cold acetonitrile containing fluconazole as an internal standard. Stability data were expressed in % drug remaining *vs* time graph considering 0 min area ratio as 100%.

The analysis of compound **6f** was done by API 3200 LC-MS/MS using positive MRM mode. Chromatographic separation was achieved using Waters symmetry, C18, 4.6 ×150 mm, 5 μm, analytical column at ambient temperature. The mobile phase mixture consisted of 0.1 % formic acid : acetonitrile (20:80, v/v) at a flow rate of 0.7 mL/min. Injection volume kept 30μL. Total analysis time of single injection was 4.0 min. The retention time of compound **6f** (524.3 /183.2 m/z) and fluconazole as a IS (307.00/238.10 m/z) were 2.98 and 2.08 min respectively. Fig. 7A shows the representative chromatograms of compound **6f** and fluconazole (IS).

5.2.11. *In-vitro* metabolic study of compound 6f in hamster liver microsomes

The *in-vitro* metabolism studies of compound **6f** carried out in male golden Syrian hamster liver microsomes (HLM) to access *in-vitro* hepatic intrinsic clearance which could be used to predict *in-vivo* hepatic clearance in early drug discovery.[29] The metabolic reaction mixture consist of drug (1μm), microsomal protein 1.0 mg/mL, 2.0 mM nicotinamide adenine dinucleotide phosphate (NADPH), 20 mM $MgCl_2$ and quantity sufficient of Tris–HCl buffer (50 mM, pH 7.4). The total volume of incubation was 1.0 mL and the reaction mixtures were incubated at 37 °C in a bench-top Lab-Line shaker (Julabo sw

View Article Online
DOI: 10.1039/C6MD00447D

23) for 60 min. The incubation without addition of NADPH was used as a control. Testosterone was used as positive control. The metabolic reaction was initiated by adding drug after initial 10 min pre-incubation and sampling points were taken at 5, 10, 20, 40 and 60 min. 100 µL of samples were collected and mixed with 300 µL of ACN containing IS (fluconazole 1 µg/mL) in a centrifuge tube. Samples were centrifuged at approximately 12,000 g for 15 min and 120 µL of the supernatant was transferred into an injection vial for LC-MS/MS analysis. The *in vitro* half-life ($t_{1/2}$, min) and intrinsic clearance were calculated by using following equations.

$$T_{1/2} = \frac{0693}{K\ (min^{-1})}$$

$$\text{Intrinsic Clearance } (CL_{int}) = k\ (min^{-1}) X\ \frac{\text{volume of incubation (mL)}}{\text{protien in the incubation(mg)}}$$

5.2.12. Plasma protein binding study using equilibrium dialysis method

PPB study was performed in Hamster plasma at 10 µm concentrations by using equilibrium dialysis method.[30] Dialysis blocks were coated with SIGMACOTE® (Chlorinated organopolysiloxane in heptane) before the study to avoid any non-specific binding of the drug with the apparatus. Dialysis membrane (12–14 kDa molecular weight cut-off) purchased from Himedia was activated as per manufacturer's protocol.

PPB was conducted in single freeze-thawed hamster plasma. Initially, the plasma pH was adjusted to 7.4 by using either 1.0 N hydrochloric acid or 0.1 N NaOH. Then, compound **6f** was spiked at study concentration in hamster plasma (n = 6) and incubated for 30 min to ensure maximum binding to plasma proteins. After incubation spiked plasma was kept on donor side and 100 mM tris buffer (pH 7.4) was kept (n=3) on receiver side. After filling donor and receiver chambers, blocks were kept in a shaking water bath for 10 hr at 60 rpm and 37 °C. After completion of dialysis, the resulting plasma and buffer dialysates were recovered from the cells and analyzed by LC–MS/MS. Extraction of drug plasma and buffer was carried out by simple protein precipitation with acetonitrile containing 0.1% formic acid along with IS. In all the protein binding steps, organic content for spiking solution was kept 1 %. Protein binding was calculated by using following equation

$$\%\ \text{bound} = \frac{(\text{conc. in donor cell}) - (\text{conc. in receiver cell})}{\text{conc. in donor cell}} \times 100\ \%$$

5.2.13. Docking study

To know the binding mode of these series of compounds, we have subjected them to the docking into the crystal structure of hLig1. The crystal structure of hLig1 was retrieved from the PDB database (PDB ID:1X9N).[31] To prepare this structure for the docking experiments, we have removed the co-crystallized nicked DNA and Adenosine Monophosphate. This step was followed by the addition of hydrogen atoms to the protein. Then energy minimization was then performed using the Sybyl7.1.[32] The details of the structure preparation and docking procedure can be found elsewhere in the literature.[16] The structures of the compounds were drawn in sketch module incorporated in sybyl7.1. All the docking experiments were carried out using FlexX module of Sybyl7.1.[33]

Acknowledgements

The authors are grateful to the Director, CSIR-CDRI for her constant support and encouragement, Dr S. P. Singh for technical support, SAIF for NMR, IR, and Mass spectral data. The CSIR, New Delhi, is thanked for the award of Senior Research Fellowship to L.R.S, M.S, S.S, and T.S.L. This is CDRI communication number 186/2016/KVS.

Notes and references

‡Footnotes relating to the main text should appear here. These might include comments relevant to but not central to the matter under discussion, limited experimental and spectral data, and crystallographic data.

§

§§

etc.

1. J. J. Blow and R. A. Laskey, *Nature*, 1988, **332**, 546-548.
2. K. W. Caldecott, *Nat. Rev. Genet.*, 2008, **9**, 619-631.
3. a) R. Okazaki, T. Okazaki, K. Sakabe, K. Sugimoto and A. Sugino, *Proc. Natl. Acad. Sci. U S A*, 1968, **59**, 598-605; b) I. R. Lehman, *Science*, 1974, **186**, 790-797; c) F. Fabre and H. Roman, *Proc. Natl. Acad. Sci. U S A*, 1979, **76**, 4586-4588; d) C. Prigent, M. S. Satoh, G. Daly, D. E. Barnes and T. Lindahl, *Mol. Cell Biol.*, 1994, **14**, 310-317; e) A. E. Tomkinson, S. Vijayakumar, J. M. Pascal and T. Ellenberger, *Chem. Rev.*, 2006, **106**, 687-699.
4. J. M. Pascal, P. J. O'Brien, A. E. Tomkinson and T. Ellenberger, *Nature*, 2004, **432**, 473-478.
5. D. S. Levin, A. E. McKenna, T. A. Motycka, Y. Matsumoto and A. E. Tomkinson, *Curr. Biol.*, 2000, **10**, 919-922.
6. a) L. M. Henderson, C. F. Arlett, S. A. Harcourt, A. R. Lehmann and B. C. Broughton, *Proc. Natl. Acad. Sci. U S A*, 1985, **82**, 2044-2048; b) D. E. Barnes, A. E. Tomkinson, A. R. Lehmann, A. D. B. Webster and T. Lindahl, *Cell*, 1992, **69**, 495-503; c) S. Das-Bradoo, H. D. Nguyen, J. L. Wood, R. M. Ricke, J. C. Haworth and A. K. Bielinsky, *Nat. Cell Biol.*, 2010, **12**, 74-79; sup pp 71-20.
7. D. Y. Sun, R. Urrabaz, M. Nguyen, J. Marty, S. Stringer, E. Cruz, L. Medina-Gundrum and S. Weitman, *Clin. Cancer Res.*, 2001, **7**, 4143-4148.
8. a) M. Srivastava, M. Nambiar, S. Sharma, S. S. Karki, G. Goldsmith, M. Hegde, S. Kumar, M. Pandey, R. K. Singh, P. Ray, R. Natarajan, M. Kelkar, A. De, B. Choudhary and S. C. Raghavan, *Cell*, 2012, **151**, 1474-1487; b) D. Mandalapu, D. K. Singh, S. Gupta, V. M. Balaramnavar, M. Shafiq, D. Banerjee and V. L. Sharma, *RSC Adv.*, 2016, **6**, 26003-26018.
9. P. Samadder, R. Aithal, O. Belan and L. Krejci, *Pharmacol. Ther.*, 2016, **161**, 111-131.
10. B. V. Palmer, G. A. Walsh, J. A. McKinna and W. P. Greening, *Br. Med. J.*, 1980, **281**, 1594-1597; b) K. S. Chan, C. G. Koh and H. Y. Li, *Cell Death Dis.*, 2012, **3**, e411.
11. B. Bahrami, T. Greenwell and J. S. Muecke, *Clin. Exp. Ophthalmol.*, 2014, **42**, 317-322.
12. a) S. Hoelder, P. A. Clarke and P. Workman, *Mol. Oncol.*, 2012, **6**, 155-176; b) A. Kamb, S. Wee and C. Lengauer, *Nat. Rev. Drug Discov.*, 2007, **6**, 115-120.
13. G. Menchon, O. Bombarde, M. Trivedi, A. Negrel, C. Inard, B. Giudetti, M. Baltas, A. Milon, M. Modesti, G. Czaplicki and P. Calsou, *Sci. Rep-Uk*, 2016, **6**.

View Article Online
DOI: 10.1039/C6MD00447D

14. S. Howard, N. Amin, A. B. Benowitz, E. Chiarparin, H. F. Cui, X. D. Deng, T. D. Heightman, D. J. Holmes, A. Hopkins, J. Z. Huang, Q. Jin, C. Kreatsoulas, A. C. L. Martin, F. Massey, L. McCloskey, P. N. Mortenson, P. Pathuri, D. Tisi and P. A. Williams, *ACS Med. Chem. Lett.*, 2013, **4**, 1208-1212.
15. a) S. S. Stokes, M. Gowravaram, H. Huynh, M. Lu, G. B. Mullen, B. Chen, R. Albert, T. J. O'Shea, M. T. Rooney, H. Hu, J. V. Newman and S. D. Mills, *Bioorg. Med. Chem. Lett.*, 2012, **22**, 85-89; b) S. S. Stokes, H. Huynh, M. Gowravaram, R. Albert, M. Cavero-Tomas, B. Chen, J. Harang, J. T. Loch, 3rd, M. Lu, G. B. Mullen, S. Zhao, C. F. Liu and S. D. Mills, *Bioorg. Med. Chem. Lett.*, 2011, **21**, 4556-456; c) E. T. Buurman, V. A. Laganas, C. F. Liu and J. I. Manchester, *ACS Med. Chem. Lett.*, 2012, **3**, 663-667.
16. a) M. Shameem, R. Kumar, S. Krishna, C. Kumar, M. I. Siddiqi, B. Kundu and D. Banerjee, *Chem-Biol. Interact.*, 2015, **237**, 115-124; b) S. Krishna, D. K. Singh, S. Meena, D. Datta, M. I. Siddiqi and D. Banerjee, *J. Chem. Inf. Model*, 2014, **54**, 781-792.
17. a) K. V. Sashidhara, S. R. Avula, V. Mishra, G. R. Palnati, L. R. Singh, N. Singh, Y. S. Chhonker, P. Swami, R. S. Bhatta and G. Palit, *Eur. J. Med. Chem.*, 2015, **89**, 638-653; b) K. V. Sashidhara, G. R. Palnati, L. R. Singh, A. Upadhyay, S. R. Avula, A. Kumar and R. Kant, *Green Chem.*, 2015, **17**, 3766-3770.
18. a) K. V. Sashidhara, S. R. Avula, P. K. Doharey, L. R. Singh, V. M. Balaramnavar, J. Gupta, S. Misra-Bhattacharya, S. Rathaur, A. K. Saxena and J. K. Saxena, *Eur. J. Med. Chem.*, 2015, **103**, 418-428; b) K. V. Sashidhara, R. K. Modukuri, P. Jadiya, K. B. Rao, T. Sharma, R. Haque, D. K. Singh, D. Banerjee, M. I. Siddiqi and A. Nazir, *ACS Med. Chem. Lett.*, 2014, **5**, 1099-1103; c) K. V. Sashidhara, R. K. Modukuri, P. Jadiya, R. P. Dodda, M. Kumar, B. Sridhar, V. Kumar, R. Haque, M. I. Siddiqi and A. Nazir, *ChemMedChem*, 2014, **9**, 2671-2684.
19. K. V. Sashidhara, L. R. Singh, D. Choudhary, A. Arun, S. Gupta, S. Adhikary, G. R. Palnati, R. Konwar, R. Trivedi, *RSC Adv.*, 2016, **6**, 80037-80048.
20. K. V. Sashidhara, G. R. Palnati, R. P. Dodda, S. R. Avula and P. Swami, *Synlett*, 2013, **24**, 1795-1800.
21. M. W. Beukers, M. J. Wanner, J. K. V. Kunzel, E. C. Klaasse, A. P. IJzerman and G. J. Koomen, *J. Med .Chem.*, 2003, **46**, 1492-1503.
22. a) A. Y. Lukmantara, D. S. Kalinowski, N. Kumar and D. R. Richardson, *Org. Biomol. Chem.*, 2013, **11**, 6414-6425. b) L. Tripathi and P. Kumar, *Eur. J. Med. Chem.*, 2013, **64**, 477-487; c) J. F. de Oliveira, A. L. da Silva, D. B. Vendramini-Costa, C. A. da Cruz Amorim, J. F. Campos, A. G. Ribeiro, R. Olimpio de Moura, J. L. Neves, A. L. Ruiz, J. Ernesto de Carvalho and C. Alves de Lima Mdo, *Eur. J. Med. Chem.*, 2015, **104**, 148-156.
23. D. K. Singh, S. Krishna, S. Chandra, M. Shameem, A. L. Deshmukh and D. Banerjee, *Med. Res. Rev.*, 2014, **34**, 567-595.
24. J. Montero, C. Dutta, D. van Bodegom, D. Weinstock and A. Letai, *Cell Death Differ.*, 2013, **20**, 1465-1474.
25. H. Teraoka, H. Minami, S. Iijima, K. Tsukada, O. Koiwai and T. Date, *J. Biol. Chem.*, 1993, **268**, 24156-24162.
26. R. L. A. Furlan, L. M. Garrido, G. Brumatti, G. P. Amarante-Mendes, R. A. Martins, M. C. R. Facciotti and G. Padilla, *Biotechnol. Lett.*, 2002, **24**, 1807-1813.
27. J. B. LePecq and C. Paoletti, *J. Mol. Biol.*, 1967, **27**, 87-106.
28. C. D. Bevan and R. S. Lloyd, *Anal. Chem.*, 2000, **72**, 1781-1787.
29. P. Baranczewski, A. Stanczak, K. Sundberg, R. Svensson, A. Wallin, J. Jansson, P. Garberg and H. Postlind, *Pharmacol. Rep.*, 2006, **58**, 453-472.
30. H. Chandasana, Y. S. Chhonker, V. Bala, Y. D. Prasad, T. K. Chaitanya, V. L. Sharma and R. S. Bhatta, *J. Chromatogr. B. Analyt. Technol. Biomed. Life Sci.*, 2015, **985**, 180-188.
31. J. M. Pascal, P. J. O'Brien, A. E. Tomkinson and T. Ellenberger, *Nature*, 2004, **432**, 473-478.
32. Sybyl, version 7.1; Tripos, Inc.: St. Louis, MO, 2005.
33. M. Rarey, B. Kramer, T. Lengauer and G. Klebe, *J. Mol. Biol.*, 1996, **261**, 470-489.

View Article Online
DOI: 10.1039/C6MD00447D

Table of Contents:

Design, synthesis and anticancer activity of dihydropyrimidinone-semicarbazone hybrids as potential Human DNA Ligase1 inhibitors

Koneni V. Sashidhara,[a,*] L. Ravithej Singh,[†,a] Mohammad Shameem,[†,b] Sarika Shakya,[a] Anoop Kumar,[a] Tulsankar Sachin Laxman,[c] Shagun Krishna,[b] Mohammad Imran Siddiqi,[b] Rabi S. Bhatta[c] and Dibyendu Banerjee[b]

[a]*Medicinal and Process Chemistry Division,* [b]*Molecular and Structural Biology Division,* [c]*Pharmacokinetics and Metabolism Division, CSIR-Central Drug Research Institute, BS-10/1, Sector 10, Jankipuram Extension, Sitapur Road, Lucknow, 226031, India.*

[†]*These authors contributed equally.*

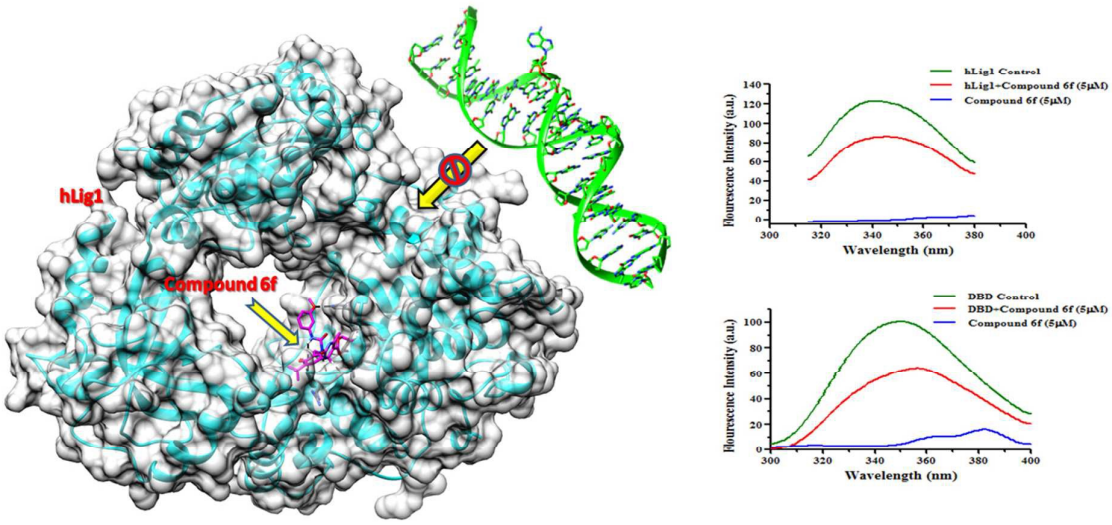

A series of rationally designed new class of human DNA ligase1 inhibitors with potent *in-vitro* anti-cancer properties is presented.